Phonon-mediated unconventional superconductivity in strongly correlated systems

Georgios Varelogiannis*
Institute of Electronic Structure and Laser, Foundation for Research and Technology—Hellas, P.O. Box 1527, Heraklion Crete 71110, Greece
(Received 26 June 1997)

We propose an adiabatic approach for Hubbard models in the Fermi-liquid regime coupled to phonons. The Hubbard parameters are associated with the bandwidth W via an interpolation formula between the trivial for W strong- and weak-coupling limits of Hubbard models. Phonons are introduced via an adiabatic random-phase approximation scheme. We obtain simple conditions for phonon-driven instabilities in a Fermi liquid with short-ranged interactions. We report phonon-driven instabilities without nesting and describe the elimination of the Peierls instability in a nested system by Coulomb correlations. We also report the possibility for a phonon-driven phase separation (PS) instability as well as the strong enhancement of forward processes in the effective electron-phonon scattering near the phase separation instability. We show that the proximity to PS induces momentum decoupling (MD) in superconductivity which implies a tendency for decorrelation between the physics in the different regions of the Fermi surface. MD could induce anisotropic superconductivity with unconventional gap symmetry such as d wave. Whether anisotropy in the high-T_c oxides is driven by MD or by anisotropic scattering (for example with spin fluctuations) becomes a crucial question. We discuss some qualitative implications of MD that explain puzzling qualitative aspects of superconductivity in the oxides and could advocate that MD is at the origin of anisotropies. Such effects are the marginality of the superconducting gap symmetry for the condensation free energy and the resulting possibility of gap symmetry transitions with the doping, the temperature dependence of the shape of the anisotropy, and the behavior of the anomalous dip above the gap in the density of states. We also show that in the MD regime the orthorhombic distortion of the CuO_2 planes in $YBa_2Cu_3O_7$ could be sufficient to explain the mixing of s-gap components in the dominantly d-wave gap. On the other hand, if spin fluctuations mediate the pairing in $YBa_2Cu_3O_7$, at least 25% of the condensate must be located in the chains. Our analysis could rehabilitate phonons as potential mediators of the pairing in all ''unconventional'' superconductors including heavy-fermion and organic compounds. [S0163-1829(98)06914-8]

I. INTRODUCTION

Despite the intense theoretical activity, there is no consensus on the microscopic mechanism responsible for high-T_c superconductivity. Many authors argue that Coulomb correlations or magnetic interactions are at the origin of high-T_c. To understand the effect of strong Coulomb correlations of the carriers in cuprates, a first step is the understanding of the behavior of the Hubbard model at strong couplings. Considerable theoretical activity has been devoted to the study of models derived from the Hubbard model involving sophisticated numerical and field-theoretical methods[1–3] and allowing significant progress. However, the study of Coulomb correlations alone may not be sufficient in the oxides. Various experiments like neutron diffraction,[4] Raman spectroscopies,[5] site-selective isotope effect measurements,[6] and tunneling,[7] indicate that phonons are probably strongly coupled to the carriers, and may also play an important role in the mechanism that leads to high-T_c.[8]

In this spirit, much attention has been attracted recently by models in which electron-phonon coupling and strong Coulomb correlations are simultaneously present.[9–15] In some of these approaches, a Hubbard model with an additional local (Holstein) electron-phonon coupling term was considered.[10,14,15] The presence of phonons complicates further the strongly correlated electronic problem. On the other hand, including a phonon term in the Hubbard Hamiltonian implies somehow the constraint to treat phonons on the same footing with the electronic terms and this is by definition a nonadiabatic approach which complicates tremendously the eventual study of superconductivity. In this manuscript, we adopt a simpler approach to Hubbard models in the presence of adiabatic electron-phonon coupling, being consistent with the following analysis of the resulting superconductivity within a BCS framework. The electron-phonon scattering is supposed adiabatic *ab initio*, treating therefore the questions of Coulomb correlations and electron-phonon correlations separately.

Our approach can be sketched as follows. The electron-phonon coupling is considered as adiabatic *ab initio* in the sense that it is not interfering with the electronic degrees of freedom. The first step is the link between the relevant parameters of the Fermi liquid and the parameters of the Hubbard models without electron-phonon coupling. We show that the knowledge of the bandwidth W is sufficient for our purpose. Having made this remark, the link between the Fermi liquid and Hubbard parameters is greatly simplified. In fact, W is obtained rather trivially in the weak-coupling and strong-coupling limits of the Hubbard model. We assume that W has a smooth crossover from its strong-coupling to its weak-coupling behavior and describe it by a simple interpolation formula. We obtain, therefore, W for any magnitude of the Coulomb correlations. This simple interpolation formula describes reasonably the behavior of W, as can be seen by comparing with numerical exact diagonalization results from which we can even estimate the parameters of our interpola-

tion formula. Phonons are introduced via an adiabatic random-phase approximation (RPA) scheme, which leads to an effective composite interaction. In this way we avoid the complications with nonadiabaticity mentioned above, without losing relevant physics. The strength of the electron-phonon coupling is treated as a phenomenological free parameter that can be obtained analyzing characteristic experiments.[16,17] We could say that the spirit of our analysis is somewhat similar to that of Overhauser on the exchange effects in a correlated electron gas.[18]

We must insist here on the fact that our approach deliberately neglects the rich magnetic physics of Hubbard type models. We suppose in fact, without proving it, that the behavior of the charge degrees of freedom is sufficient as far as the electron-phonon problem is concerned. However, it appears quite probable to us that the charge instabilities will be accompanied by spin instabilities. This could indicate that one cannot exclude *a priori* interference of magnetic degrees of freedom with electron-phonon scattering. Simplicity is in fact the only justification of our approach. Reversing the argument, we could say that if a complete heavy treatment of the lattice Hamiltonian is adopted in the Fermi-liquid regime, then it is worth considering the interference of the magnetic degrees of freedom with electron-phonon scattering. Otherwise, for the charge degrees of freedom our simple approach is to a large extent sufficient.

Within our approach we can describe the conditions under which the phonon-driven charge instabilities may occur. The novelty of Hubbard Fermi liquids is precisely the possibility to undergo phase separation (PS) instability due, for example, to electron-phonon coupling, that in ''normal'' (free-electron-gas-like) Fermi liquids is eliminated by the long-range character of Coulomb correlations. We can clearly see within our approach that close to the PS instability the effective interaction of the carriers with optical phonons is strongly enhanced at forward scattering. Dominance of forward processes in the effective scattering leads to momentum decoupling (MD) in superconductivity. In the MD regime even *phonon-mediated superconductivity has very ''unconventional'' properties* that could explain many qualitative puzzling aspects of the superconducting phenomenology of the high-T_c oxides. In particular, the proximity of a phase separation instability becomes an alternative to anisotropic scattering (for example with spin fluctuations) explanation of anisotropic superconductivity of s- or d-wave gap symmetry. It becomes, therefore, a crucial problem to distinguish whether anisotropies in the superconductive behavior of high-T_c oxides, and especially d waves, are due to momentum decoupling or due to anisotropic scattering, for example, in a conventional approach, with antiferromagnetic spin fluctuations. We analyze some qualitatively puzzling aspects of the phenomenology of the oxides that advocate momentum decoupling as the origin of anisotropic superconductivity in the cuprates.

Momentum decoupling does not necessarily imply proximity of phase separation instability. There are alternative theoretical approaches that could lead to a similar situation for the superconductive behavior. For example, the interlayer tunneling pairing model proposed by Anderson is effectively $q \approx 0$ pairing.[19] The proposed pairing mediated by a charge-transfer resonance[20] is also based on small-q processes.[21] It is also possible that the two-dimensional structure of the electronic system favors forward scattering with some optical phonons.[22] We do not claim here a demonstration that instabilities are phonon driven in the oxides. Whatever the origin of the phase separation instability, in its vicinity the interaction of the electronic system with any bosonic field will be dominated by forward scattering and therefore momentum decoupling occurs. Also our simple approach is not expected to capture all the relevant physics of the oxides. We are rather considering this case as a paradigm for a phase separation instability in a strongly correlated system for which we are able to apply a simple theoretical approach and show that phonon-dominated physics may concern various unconventional parts of the phenomenology of the oxides.

It results from our analysis that while ''simple'' phonon mechanisms must be excluded for the oxides, when the electronic system is close to the PS instability the interaction of electrons with phonons deserves serious consideration in connection with the high-T_c phenomenon. In fact, the combination of MD and extended van Hove singularities may also reconcile many of the experimental arguments (other than anisotropies) used in the past to exclude phonons, like the weakness of the isotope effect in optimally doped oxides,[23] the linear temperature dependence of the dc resistivity,[24] etc. On the other hand, the noticeable isotope effect away from optimal doping[25] is very difficult to reconcile with mechanisms where phonons are totally absent[26] and can be considered as an additional argument that the mechanism of MD with phonons presented here, is a serious candidate that merits careful investigations.

The paper is organized as follows. In Sec. II, we briefly describe the adiabatic RPA scheme that leads to the effective composite interaction. We show how phonon-driven instabilities and in particular PS occur in this formalism. In Sec. III, we show how, in our case, using a simple interpolation formula for the dependence of the bandwidth W on the Hubbard parameters, we can make the link between Fermi-liquid parameters and Hubbard parameters. In Sec. IV, we describe the conditions under which phonon-driven instabilities occur in a Hubbard model. In Sec. V, we show that approaching the instability line from the Fermi-liquid regime, we have precursors of the instability in the effective scattering amplitude. In particular, forward-scattering processes are strongly enhanced which results in an effective momentum cutoff in the scattering amplitude. In Sec. VI, we show that in the vicinity of the phase separation instability, the dominance of forward scattering induces momentum decoupling in superconductivity leading to anisotropies driven by the angularly resolved electronic density of states (ARDOS) even if the scattering is isotropic. Discerning whether anisotropies in the superconducting properties of the oxides and d-wave gaps, are due to momentum decoupling or to anisotropic scattering becomes a crucial question for understanding their physics. In Sec. VII, we discuss some fundamental qualitative points that may answer the question of the origin of anisotropies. We show that the doping-induced variation of the gap symmetry and the observation of different gap symmetries in different oxides (Sec. VII A), the temperature dependence of the shape of the anisotropy (Sec. VII B), and the behavior of the anomalous dip structure above the gap in tunneling and angle-resolved photoemission spectroscopy (ARPES) (Sec. VII C), are puzzling aspects advocating momentum decoupling in high-T_c oxides. We also show that one can obtain an

indirect answer to the question of the origin of the anisotropies in superconductivity by answering the question of the relevance of the chains in Y-Ba-Cu-O, since only in the momentum decoupling regime the orthorhombicity distortion of the CuO_2 planes may be sufficient to explain the mixing of s- and d-wave gap components (Sec. VII D). Finally, in Sec. VIII, we summarize our conclusions.

II. THE EFFECTIVE COMPOSITE INTERACTION

The effective interaction is the sum of the Coulomb and the electron-phonon interaction. Since our approach is adiabatic, the Coulomb interaction is taken instantaneous and there is no need for a propagator to be associated with the Coulomb lines, instead we can use an effective scalar repulsion V. On the other hand, the electron-phonon interaction is retarded and therefore we consider both the phonon propagator and the electron-phonon vertex. To introduce screening, we must renormalize by polarization effects the Coulomb repulsion, the phonon propagator and the electron-phonon vertex. Notice that, in accordance with our adiabatic assumption, while the phonon propagator and the electron-phonon vertex are renormalized by Coulomb effects, the Coulomb part is not affected by the electron-phonon interaction.

The effective composite interaction reads

$$\Lambda(\mathbf{q},\omega)=V^{\mathrm{eff}}(\mathbf{q},\omega)+[g^{\mathrm{eff}}(\mathbf{q},\omega)]^2\mathcal{D}^{\mathrm{eff}}(\mathbf{q},\omega), \tag{1}$$

where $V^{\mathrm{eff}}(\mathbf{q},\omega)$ is the effective Coulomb repulsion given by

$$V^{\mathrm{eff}}(\mathbf{q},\omega)=V(\mathbf{q},\omega)+V^{\mathrm{eff}}(\mathbf{q},\omega)\Pi(\mathbf{q},\omega)V(\mathbf{q},\omega) \tag{2}$$

the effective phonon propagator $\mathcal{D}^{\mathrm{eff}}(\mathbf{q},\omega)$ is given by

$$\mathcal{D}^{\mathrm{eff}}(\mathbf{q},\omega)=\mathcal{D}^{0}(\mathbf{q},\omega)+\mathcal{D}^{\mathrm{eff}}(\mathbf{q},\omega)\Pi(\mathbf{q},\omega)g^2\mathcal{D}^{0}(\mathbf{q},\omega)+\mathcal{D}^{\mathrm{eff}}(\mathbf{q},\omega)\Pi^2(\mathbf{q},\omega)g^2V^{\mathrm{eff}}(\mathbf{q},\omega)\mathcal{D}^{0}(\mathbf{q},\omega), \tag{3}$$

and the effective electron-phonon interaction g^{eff} is given by

$$g^{\mathrm{eff}}(\mathbf{q},\omega)=g+V^{\mathrm{eff}}(\mathbf{q},\omega)\Pi(\mathbf{q},\omega)g. \tag{4}$$

The parameter $\Pi(\mathbf{q},\omega)$ represents the polarization part and the ''free'' phonon propagator $\mathcal{D}^{0}(\mathbf{q},\omega)$ is defined by

$$\mathcal{D}^{0}(\mathbf{q},\omega)=\frac{\Omega_{\mathbf{q}}}{\omega^2-\Omega_{\mathbf{q}}^2}. \tag{5}$$

Replacing Eqs. (2)–(5) in Eq. (1), the effective composite interaction takes the following form:

$$\Lambda(\mathbf{q},\omega)=\frac{V(\mathbf{q},\omega)}{P(\mathbf{q},\omega)}+\frac{\tilde{g}^{\,2}(\mathbf{q},\omega)}{P(\mathbf{q},\omega)}\times\frac{2\Omega_{\mathbf{q}}^2}{\omega^2P(\mathbf{q},\omega)-\Omega_{\mathbf{q}}^2[P(\mathbf{q},\omega)-\tilde{g}^2(\mathbf{q},\omega)\Pi(\mathbf{q},\omega)]}, \tag{6}$$

where $P(\mathbf{q},\omega)=1+V(\mathbf{q},\omega)\Pi(\mathbf{q},\omega)$. With this notation the Coulomb interaction $V(\mathbf{q},\omega)$ is positive and $\tilde{g}^{\,2}=g^2/\Omega_{\mathbf{q}}$, where g is the bare electron-phonon scattering.

The above is generally true for a Fermi liquid irrespective of the geometry of the system or the exact mechanism and structure of Coulomb correlations. Supposing that a Hubbard model captures the physics of the Coulomb correlations of the carriers, we assume essentially that Coulomb correlations have the peculiarity of being short range, as opposed to the infinite range Coulomb correlations in a simple electron gas. The novelty when the long-range part is neglected is the possibility for the system to undergo phase separation instability. Various magnetic and charge instabilities of Coulombic origin have been reported in the literature in Hubbard-type models.[27–31] Here, we consider instabilities due to the presence of the electron-phonon interaction which we call phonon-driven instabilities. Phonon-driven instabilities have also been discussed in Refs. 13 and 15 on the basis of a slave-boson approach to a Hubbard Hamiltonian in the $U/t\rightarrow\infty$ regime with a local Holstein electron-phonon term.

An instability corresponds to a divergence of the effective composite interaction Λ. If the instability is Coulomb driven, then it comes from the first term of Eq. (6), while a phonon-driven instability is due to a singularity in the second term. Taking the $\omega\rightarrow0$ limit of Eq. (6), we can see that a phonon-driven instability appears when the following condition is fulfilled:

$$1+V(\mathbf{q},0)\Pi(\mathbf{q},0)-\tilde{g}^{\,2}\Pi(\mathbf{q},0)=0. \tag{7}$$

In the random-phase approximation (RPA) scheme the polarization part $\Pi(\mathbf{q},\omega)$ is replaced by the bare or Linhardt bubble $\Pi_0(\mathbf{q},\omega)$. This last approximation is supposed to give a rather good description in the long-wavelength limit where the exchange interaction is neglected compared to the direct Coulomb interaction. As we are going to see in the following, the RPA scheme is suitable for systems that are close to the phase separation (PS) instability, since in that case, the physics is indeed dominated by long-wavelength processes. In fact, a PS instability is an instability at $q\rightarrow0$ and near this instability the system is very susceptible to any long-wavelength process. In a classical electron gas the long-range part of the Coulomb interaction implies a $1/q^2$ divergence of $V(\mathbf{q}\rightarrow0,0)$ and therefore phonon-driven PS instabilities are impossible since the condition of Eq. (7) cannot be fulfilled when $q\rightarrow0$. On the other hand, when the Coulomb interaction is local like in Hubbard models, this is reflected in the residual Coulomb interactions of the carriers by a finite value even when $q\rightarrow0$. To establish, therefore, the vocabulary, we will call a Fermi liquid with short-ranged interactions (of Hubbard type) a system in which $V(\mathbf{q}\rightarrow0,0)$ is finite as opposed to a ''normal'' (free-electron-like) Fermi liquid in which $V(\mathbf{q}\rightarrow0,0)\rightarrow\infty$.

To get a qualitative insight let us replace the bubble by the Linhardt function. The Linhardt bubble at $\omega=0$ reads

$$\Pi_0(q,\omega=0)=N(E_F)F(q/2k_F), \tag{8}$$

where

$$F(x)=1+\frac{1}{2x}(1-x^2)\ln\left|\frac{1+x}{1-x}\right|. \tag{9}$$

Therefore, the condition for an instability given in Eq. (7) reads

$$V(q,\omega=0)=\tilde{g}^2-\frac{1}{N(E_F)F(q/2k_F)}. \tag{10}$$

We remark that $1/F(q/2k_F)$ grows smoothly for $q\leqslant 2k_F$, while for $q>2k_F$ it grows rapidly behaving approximatively as

$$\left.\frac{1}{F(x)}\right]_{x\gg 1}\approx\frac{3x^2}{2}-\frac{3}{10}+O\left(\frac{1}{x}\right). \tag{11}$$

Monotonic growth of $\Pi_0^{-1}(q,\omega=0)$ in the small-q region is still true even if the bubble is calculated for tight-binding two-dimensional models that are supposed to describe the electronic structure of high-T_c oxides. This is going to be the case later (in Sec. V) where we discuss the possible applicability of some of our results to the oxides. Since $F^{-1}(q/2k_F)$ is a monotonically growing function and $F(x=0)=2$ we can conclude from Eq. (10) that if

$$V\leqslant V^C=\tilde{g}^2-\frac{1}{2N(0)}, \tag{12}$$

then the electronic system is certainly driven to an instability because of the strong electron-phonon coupling. If $V=V^C$ the instability occurs for $q\to 0$ and it is a PS instability, while for $V<V^C$ the instability occurs at a finite momentum and corresponds to a charge-density wave (CDW) instability. As we mentioned earlier, within the RPA approach the exchange interaction is neglected compared to the direct Coulomb interaction. Therefore, we cannot trust this description for momenta of the order k_F, and since we will limit ourselves here to RPA, we will avoid discussion of CDW at large momenta. The inclusion of the exchange effects would be necessary for example in the study of magnetic effects where the relevant physics is at large momenta of the order k_F. Of course, the Coulomb repulsion $V(\mathbf{q},\omega)$ is the residual repulsion among the quasiparticles, and its relation with the on-site repulsion of a Hubbard model is not trivial and it is given from a solution of the Hubbard problem in the Fermi-liquid regime. However, for our purpose, this type of complex solution may be avoided as described in the next section.

III. FERMI LIQUID AND HUBBARD PARAMETERS

A basic problem is the link between the parameters of the considered Hubbard model and the characteristics of the resulting Fermi-liquid regime. For the $U\to\infty$ regime this can be achieved, for example, using a slave-boson approach and a $1/N$ expansion.[32] Our simple approach *cannot* replace such methods. Our aim is to give easily applicable results on the characteristics of the charge Fermi-liquid behavior, valid in the whole range of couplings of the Hubbard model. By making the serious simplification of neglecting the magnetic behavior, we avoid searching tedious solutions of the problem without losing the relevant physics.

From the Fermi-liquid point of view, the fundamental quantity related to Coulomb correlations is the bandwidth W. One naturally expects that Coulomb correlations of the carriers reduce W obtained, for example, by local-density-approximation (LDA) calculations.[33] It is noticeable that in high-T_c oxides, LDA calculations provide a reasonable description of Fermi surfaces as confirmed by angle-resolved-photoemission (ARPES) results overestimating, however, largely W. This indicates that indeed the carriers are strongly correlated.[34] In our previous analysis, W does not appear explicitly. It is, nevertheless, naturally associated with the stability of the system and at *small* doping we can see its influence through the relation

$$V\leqslant W. \tag{13}$$

Coulomb correlations tend to avoid that electrons occupy the same site and this can cost them at most the kinetic energy $\approx W$ as it is nicely explained by Fulde in Ref. 35. The smaller the Coulomb repulsion, the larger the W/V ratio, while the equality $V\approx W$ could hold only in the infinite Coulomb repulsion and the very small hole doping regime.[35,36]

From Eq. (12), we have seen that small residual Coulomb repulsion of the carriers V favors phonon-driven instabilities. From Eq. (13), this turns out to be equivalent with the statement that small bandwidth W favors phonon-driven instabilities and this is quite reasonable. In fact, if $W\leqslant V^C$ then a phonon-driven instability will certainly occur. Combining, therefore, Eqs. (12) and (13) we are already able, given the bandwidth, to provide sufficient (yet not necessary) conditions for a phonon-driven instability to occur.

Having identified that W may be the crucial parameter, Hubbard Hamiltonians become trivial in the extreme weak- and strong-coupling limits. Next we write a simple Hubbard Hamiltonian to define our notations

$$H=t\sum_{\langle i,j\rangle\sigma}a_{i\sigma}^{\dagger}a_{j\sigma}+U\sum_i n_{i\uparrow}n_{i\downarrow}, \tag{14}$$

where U is the on-site repulsion and $\langle i,j\rangle$ denotes pairs of nearest neighbors. It will be clear later that our analysis can be straightforwardly generalized to complex hopping situations and this is one of the greatest advantages of our approach.

In the extreme weak-coupling regime ($U/t\to 0$), only the kinetic term of Eq. (14) remains. Then the dispersion becomes $\varepsilon_{\mathbf{k}}=-4t\Sigma_{i=1}^{d}\cos(k_i)$ where d is the dimensionality and $W=2tz$ with $z=2d$ the number of nearest neighbors. On the other hand, in the $U/t\to\infty$ regime, double occupancy of sites is forbidden making interesting the work in a reduced Hilbert space where all configurations containing doubly occupied sites are forbidden. This is done though a Schrieffer-Wolf transformation of the Hamiltonian,[37,35] that leads to an effective Hamiltonian $\tilde{H}$ acting in the reduced Hilbert space, which in the $U/t\to\infty$ regime is reduced to an effective hoping term $\tilde{H}=t\Sigma_{\langle i,j\rangle\sigma}(\tilde{a}_{i,\sigma}^{\dagger}\tilde{a}_{j,\sigma}+\text{H.c.})$ with effective annihilation and creation operators $\tilde{a}_{j,\sigma}=a_{j,\sigma}(1-n_{j-\sigma})$ and $\tilde{a}_{i,\sigma}^{\dagger}=a_{i,\sigma}^{\dagger}(1-n_{i-\sigma})$, respectively.[35] Defining δ the hole concentration or the doping from half-filling, the effective hopping term leads, in analogy with the weak-coupling regime, to a bandwidth $W=2zt\delta$. Therefore, in the $U/t\to 0$ and $U/t\to\infty$ regimes, the bandwidth is obtained essentially *without solving the Hamiltonian*. Although in these two extreme limits W is trivial, when U/t is finite we are not able to predict W as function of the Hubbard parameters U/t, z, and δ for two-dimensional models that could be relevant for the oxides.

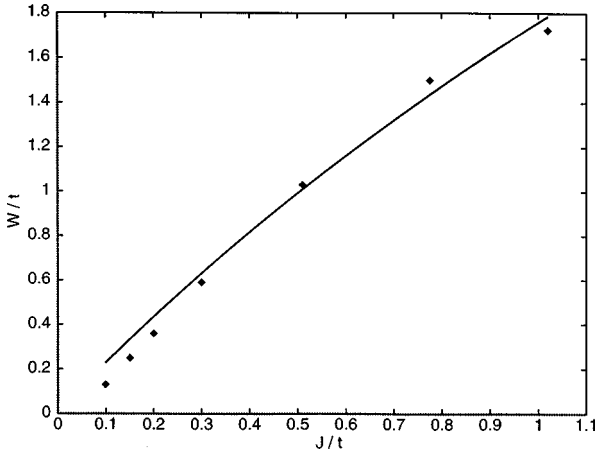

FIG. 1. The dependence of the bandwidth W/t on J/t as obtained by numerical exact diagonalization on a cluster with one hole in Ref. 39 (black dots), and from our interpolation formula Eq. (15) with $z=2$, $\mu=1$, and $a=0.28$ (full line). The results of Ref. 39 confirm our prescription of a smooth polynomial crossover from the $U/t\rightarrow 0$ to the $U/t\rightarrow\infty$ regime of the bandwidth in the Hubbard model.

Since W is a fundamental parameter for our discussion, we will try to overcome this handicap with a simple interpolation formula. We suppose that for the intermediate couplings, there is no particular resonance, and the system switches smoothly from the $U/t\rightarrow 0$ regime to the $U/t\rightarrow\infty$ regime. We propose the simplest two-parameter polynomial interpolation between the strong- and weak-coupling regime dependence of W on the Hubbard parameters

$$W=2zt\delta+\frac{2zt(1-\delta)a(J/t)^{\mu}}{1+a(J/t)^{\mu}}=2zt\delta+\frac{2zt(1-\delta)}{1+b(U/t)^{\mu}}, \tag{15}$$

where t is the hopping matrix element, U is the local repulsion in a Hubbard Hamiltonian, δ is the doping from half-filling, and z is the number of nearest neighbors ($2zt=8t$ in the two-dimensional case considered in relation to high-T_c's). This formula interpolates smoothly between the $U\rightarrow 0$ regime where $W\approx 2zt$ and the $W\rightarrow\infty$ regime where $W\approx 2zt\delta$. We remark that $J=2t^2/U$ is the well-known parameter of the t-J description of the Hubbard model (obtained after the Schrieffer-Wolf transformation mentioned previously), which implies $ab=2^{-\mu}$.

The coefficients a or b and μ can be estimated by fit to the results of numerical calculations, although, their exact values have no qualitative influence on the following discussion. In the very strong-coupling limit ($U/t\rightarrow\infty$) in a square lattice we have from Eq. (15) $W\approx 8t\delta+8t(1-\delta)a(J/t)^{\mu}$, and since various numerical simulations point to a linear dependence of the bandwidth on J/t,[38,39,2] we can choose $\mu=1$. Taking also $a\approx 0.28$, we can reasonably fit (see Fig. 1) the J/t dependence of W obtained by Poilblanc *et al.*[39] from numerical exact diagonalization on a cluster with one hole. Better fits of these last results can be obtained by taking for example $\mu=1.1$ but this is not so important for our purpose. The quality of the fit shown in Fig. 1, gives an indication on the validity of our interpolation formula, and also establishes our prescription for a smooth polynomial crossover from the strong- to the weak-coupling regimes.

Equation (15) which relates W with the parameters of the one-band Hubbard model, can be straightforwardly generalized for the case of more complex hopping situations. The advantage of our approach is to isolate the effect of the Coulomb repulsion even in the case of Hubbard models with complex hopping terms, that will just lead to an effective hopping term $\tilde{t}$ in Eq. (15). As will be made clear in the following, t sets the energy scale without interfering with our qualitative discussion. We illustrate that point in the three-band Hubbard model which is frequently used to describe the physics in the CuO_2 planes of the cuprates.[40] If the indices p and d refer to the p band and d band, respectively, then in the relevant for cuprates limit $\varepsilon_p-\varepsilon_d\gg t_{pd}$ we have $W(U\rightarrow 0)\approx 8t_{pd}^2/(\varepsilon_p-\varepsilon_d)$, while in the opposite limit $W(U\rightarrow\infty)\approx[8t_{pd}^2/(\varepsilon_p-\varepsilon_d)]\delta$.[15] Therefore, the situation is quite similar to that of the one-band Hubbard model, except that now we have an effective hopping $\tilde{t}=t_{pd}^2/(\varepsilon_p-\varepsilon_d)$. Our previous approach remains valid and the dependence of the bandwidth on the parameters of the three-band Hubbard model can be reasonably described by

$$W=\frac{2zt_{pd}^2\delta}{\varepsilon_p-\varepsilon_d}+\frac{2zt_{pd}^2(1-\delta)}{\varepsilon_p-\varepsilon_d}\frac{1}{1+b(U(\varepsilon_p-\varepsilon_d)/t_{pd}^2)^{\mu}}. \tag{16}$$

The same occurs if next-nearest neighbors and other hopping terms are included. Since our discussion is independent on the hopping behavior, our analysis is valid whatever the electronic dispersion is and many qualitative aspects of the discussion that follows are *generic*.

IV. PHONON-DRIVEN INSTABILITIES IN A FERMI LIQUID WITH SHORT-RANGED INTERACTIONS

Combining Eqs. (12), (13), and (15) gives *sufficient* (but not necessary) conditions for a phonon-driven instability of the electronic system described by the inequality

$$2zt\delta+\frac{2zt(1-\delta)a(J/t)^{\mu}}{1+a(J/t)^{\mu}}\leqslant\tilde{g}^2-\frac{1}{2N(E_F)}. \tag{17}$$

Our feeling is that nesting effects or saddle points that may lead to peaks in the density of states, would help instabilities. This is naturally contained in our analysis and we can distinguish two extreme cases with *all physical situations ranging in between.* First, we suppose that the electronic density of states is rather homogeneous all over the bands, or in other terms, there are not important nesting or saddle-point effects in the system. We are, therefore, in the less favorable situation for instabilities. In that case, there exists a simple relationship between the density of states at the Fermi level $N(E_F)$ and the bandwidth $2W\approx 1/N(E_F)$. Using this relation and Eq. (17) we obtain the following sufficient condition for instability:

$$\frac{\tilde{g}^2}{t}\geqslant\left[4z-\frac{4z}{1+b(U/t)^{\mu}}\right]\delta+\frac{4z}{1+b(U/t)^{\mu}}. \tag{18}$$

The condition for instability depends linearly on the doping δ except in the weak-coupling regime ($U/t\rightarrow 0$) where the

doping is an irrelevant parameter. In this last case, the condition for instability becomes $\tilde{g}^2/t \geqslant 4z$ and is very difficult to fulfill. Notice, however, that the smaller the number of nearest neighbors z, the easier is met the condition for instability which is a quite natural result. On the other hand, in the strong-coupling regime ($U/t \to \infty$) the border for instability is a line with slope $4z$ that crosses the origin. Whatever the electron-phonon coupling is, at sufficiently small doping a phonon-driven instability occurs even in the absence of nesting. The doping is now the relevant parameter.

We suppose now that we are in a situation of perfect nesting or with van Hove singularities on the Fermi level, which is the other extreme case expected to be the most favorable for instabilities. Nesting or saddle points may lead to a divergence of the density of states at the Fermi level $N(E_F) \to \infty$, and the sufficient (but not necessary) conditions for instability become now

$$\frac{\tilde{g}^2}{t} \geqslant \left[2z - \frac{2z}{1+b(U/t)^{\mu}} \right] \delta + \frac{2z}{1+b(U/t)^{\mu}}. \tag{19}$$

The inequality (19) is easier to fulfill than Eq. (18) in all regimes.

Equations (18) and (19) are sufficient conditions for instability, in the sense that, when they are fulfilled, the system is certainly driven to an instability. But the system could also be unstable, even, if these conditions are not fulfilled. In fact, an instability may also occur even if W is higher than V^C provided the condition $V \leqslant V^C$ is met. In order to be closer to reality, we propose a second interpolation formula to describe the relationship between the effective Coulomb interaction V and the bandwidth W.

$$V = W + \frac{U-W}{1+c(U/t)^{\nu}}, \quad \nu > 1. \tag{20}$$

This formula might essentially be valid in the small doping regime which is considered relevant for high-T_c superconductivity. Equation (20) interpolates smoothly between the $U/t \to 0$ regime where $V \approx U$ and the $U/t \to \infty$ regime where $V \approx W$ (at least in the small doping regime). We see no physical reason for an anomaly at some intermediate U/t, especially when W itself has a smooth behavior between the two ($U/t \to 0$ and $U/t \to \infty$) regimes. We must notice that a similar relationship between W and V has been reported by Kanamori[36] using the t-matrix approach $V = U(1 + U/W)^{-1}$. Kanamori's formula is almost exact in the limit of large U and small density. Kanamori's result indicates that there is indeed a smooth crossover from the weak- to the strong-coupling regime in the relationship between V and W. Kanamori's formula is an excellent approximation even if it is not formally exact as $\delta \to 0$. We adopt here Eq. (20) that is a bit more general than Kanamori's formula. As for the exact value of the parameters c and ν we are going to see that they also do not have qualitative influence on our discussion. The following qualitative discussion would not be influenced, if instead of Eq. (20), Kanamori's formula was used.

Combining Eqs. (12), (15), and (20), we can write the more precise condition for instability

$$2zt\delta + \frac{2zt(1-\delta)}{1+b(U/t)^{\mu}} + \frac{1}{c(U/t)^{\nu}} \left[U - 2zt\delta + \frac{2zt(1-\delta)}{1+b(U/t)^{\mu}} \right] \leqslant \tilde{g}^2 - \frac{1}{2N(E_F)}. \tag{21}$$

Here we also distinguish the two extreme cases of the most difficult and the easiest situation for instability, all realistic situations ranging in between depending on the details of the considered systems. The most difficult situation for instability is the case of a rather homogeneous density of states where the nesting or van Hove effects are negligible and the relationship $2W \approx 1/N(E_F)$ is reasonable. Using this last relation, the instability condition given by inequality (21) reads

$$\tilde{g}^2 \geqslant 2\left[2zt\delta + \frac{2zt(1-\delta)}{1+b(U/t)^{\mu}} \right] + \frac{1}{1+c(U/t)^{\nu}} \left[U - 2zt\delta + \frac{2zt(1-\delta)}{1+b(U/t)^{\mu}} \right]. \tag{22}$$

One can better understand the constraints imposed by inequality (22) writing it in the following form:

$$\frac{\tilde{g}^2}{t} \geqslant \left[4z - \frac{4z}{1+b(U/t)^{\mu}} - \frac{2z}{1+c(U/t)^{\nu}} + \frac{2z}{[1+c(U/t)^{\nu}][1+b(U/t)^{\mu}]} \right] \delta + \frac{4z}{1+b(U/t)^{\mu}} + \frac{U/t}{1+c(U/t)^{\nu}} - \frac{2z}{[1+c(U/t)^{\nu}][1+b(U/t)^{\mu}]}. \tag{23}$$

We plot in Fig. 2(a) the instability condition as a function of the hole concentration δ for different characteristic values of the ratio U/t in the case $z=4$ (e.g., 2D square lattice) the b and μ parameters obtained by the fit of Fig. 1, and choosing $c=1$ and $\nu=2$ to be in reasonable agreement with Kanamori's result. In Fig. 2(b), we plot the condition for instability as a function of the ratio U/t for characteristic values of the hole doping and the same parameters. For each instability line the upper part of the figure corresponds to the unstable regime and the lowest part to the Fermi-liquid regime.

We see in Fig. 2(a) that for a given ratio U/t the condition for instability depends linearly on δ. This is not specifically associated to our interpolation formulas, but it is rather due to the linear δ dependence of W in the $U/t \to \infty$ regime. However, in the weak-coupling regime ($U/t \to 0$) the slope of this linear dependence is always zero. This shows that from the weak-coupling regime where the hole concentration is totally irrelevant for the stability of the system, enhancing U/t, δ becomes a relevant parameter. In the $U/t \to 0$ regime, the instability condition is trivial $\tilde{g}^2 \geqslant 2zt$ and for realistic situations is rather difficult to fulfill. The larger is the slope, the more sensitive is the system to the doping. In the $U/t \to \infty$ regime the δ slope of the instability line that crosses zero is maximal. The fact that it crosses zero implies that in the $U/t \gg 1$ regime the system is certainly unstable by the phonons at sufficiently small δ that becomes the crucial parameter. As we can see in Fig. 2(b), the necessary electron-

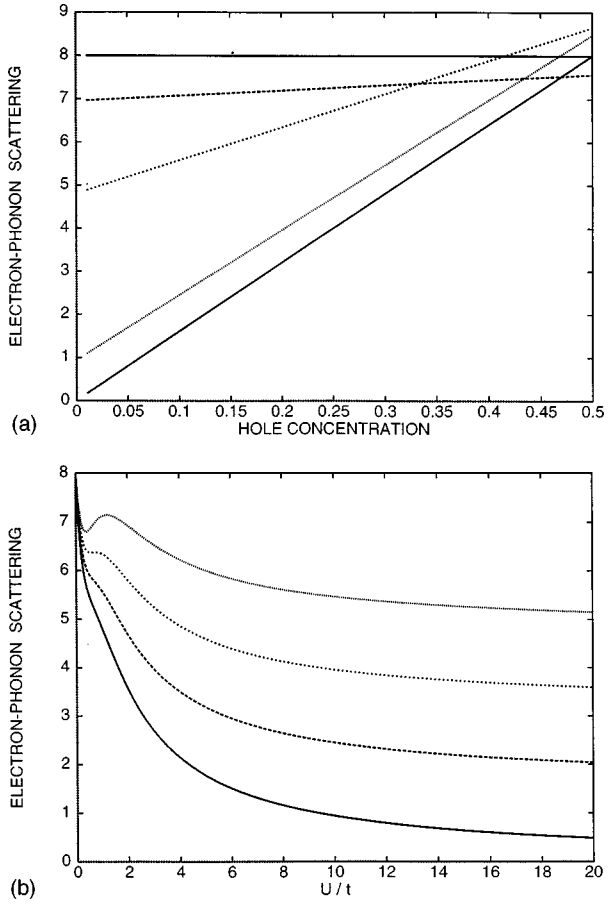

FIG. 2. (a) The critical electron-phonon scattering $\tilde{g}/t$ as a function of the hole concentration δ for a homogeneous band with $N(E_F)=1/2W$ and a square 2D lattice ($z=4$) with the coefficients b and μ obtained from the fit of Fig. 1, $c=1$ and $\nu=2$. Various U/t regimes are considered: $U/t=0$ (horizontal full line), $U/t=0.1$ (dashed line), $U/t=1$ (short dashed), $U/t=10$ (dotted) and $U/t \rightarrow \infty$ (full line that crosses origin). For each line the upper half plane corresponds to the unstable regime and the lower half plane to the Fermi-liquid regime. (b) The critical $\tilde{g}/t$ as a function of U/t for the same coefficients and various characteristic doping levels: $\delta=0$ (full line), $\delta=0.1$ (dashed line), $\delta=0.2$ (short dashed line), and $\delta=0.3$ (dotted line) (from bottom to top the doping increases). For each line, the upper half plane is always associated with the unstable regime.

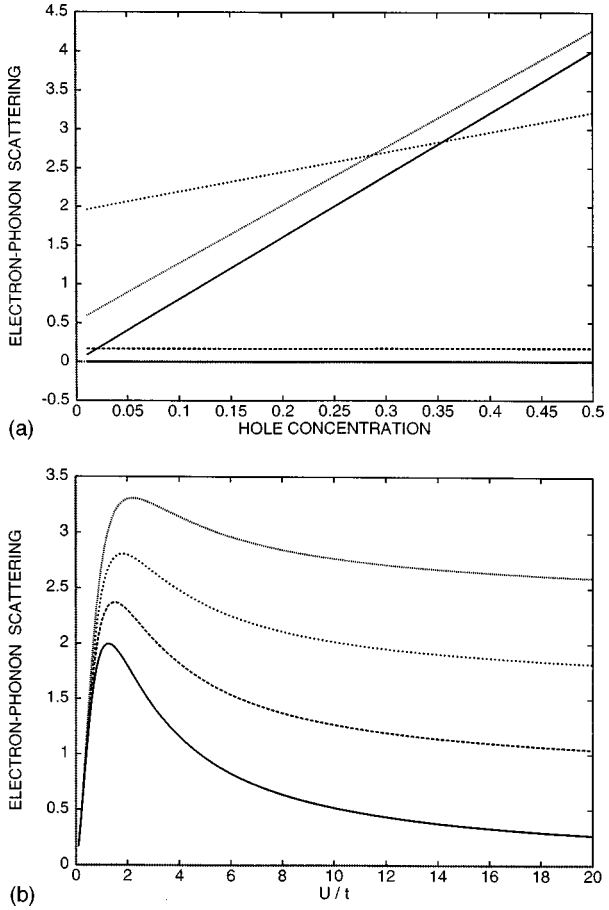

FIG. 3. (a) Same as in Fig. 2(a) but for the case $N(E_F)\rightarrow\infty$. (b) Same as in Fig. 2(b) but for the case $N(E_F)\rightarrow\infty$.

phonon coupling strength for a phonon-driven instability grows monotonically as the ratio U/t is reduced, with essentially two regimes. A rather rapid doping independent in the $U/t \leqslant 1$ region and a slower δ dependent in the $U/t \gg 1$ region. The doping always helps the system to preserve stability in the $U/t>1$ region, while is irrelevant in the $U/t<1$. From the previous remarks, we conclude that in the case of a a rather homogeneous band the instability condition is rather difficult to fulfill except in the $U/t\rightarrow\infty$ and $\delta\rightarrow 0$ situation where the electronic system is certainly driven to an instability *despite the absence of any nesting*. As we will see next, in the case of important nesting or van Hove effects the conditions for instability are much easier to fulfill and the picture changes qualitatively.

We now consider the other extreme case that could correspond, for example, to a perfect nesting. We take here $N(E_F)\rightarrow\infty$. Then the analogous to Eq. (23) condition for instability becomes

$$\frac{\tilde{g}^2}{t} \geqslant \left[2z - \frac{2z}{1+b(U/t)^{\mu}} - \frac{2z}{1+c(U/t)^{\nu}} + \frac{2z}{[1+c(U/t)^{\nu}][1+b(U/t)^{\mu}]} \right] \delta + \frac{2z}{1+b(U/t)^{\mu}} + \frac{U/t}{1+c(U/t)^{\nu}} - \frac{2z}{[1+c(U/t)^{\nu}][1+b(U/t)^{\mu}]}. \quad (24)$$

Figures 3(a) and 3(b) are the analogues of Figs. 2(a) and 2(b), the only difference being that here $N(E_F)\rightarrow\infty$. Now the situation is completely different in the $U/t\rightarrow 0$ regime. The condition for instability becomes $\tilde{g}^2/t \geqslant 0$ and is always fulfilled for a finite value of the electron-phonon coupling. In the limit of weak Coulomb correlations and $N(E_F)\rightarrow\infty$ we necessarily have phonon-driven CDW instabilities, regardless of the electron-phonon coupling strength. This instability is the well-known Peierls instability. Our approach contains naturally the possibility of a Peierls instability and this can give an indication on its validity. We can say at first that the Peierls instability occurs even if the range of the Coulomb correlations is finite provided the on-site repulsion is weak.

However, in the $U/t \to \infty$ regime the occurrence of a Peierls-type instability is not automatic. *When the ratio U/t has appreciable values, the doping becomes a relevant parameter even in the case of perfect nesting.* When $U/t \to \infty$, our previous discussion for the case of an homogeneous band remains qualitatively relevant even if nesting or van Hove effects are important. The condition for instability is, nevertheless, easier to fulfill in the case of perfect nesting, since the δ slope is twice smaller compared to that of an homogeneous band.

In this entire section we consider that the particular geometry of a given system is contained in the density of states $N(E_F)$. In fact the hopping t that appears in our formalism does not enter our qualitative discussion but sets an energy scale. Whatever the band dispersion of a given system, we may find effective tight-binding fits that could require not only nearest-neighbor but also next-nearest neighbor and other hopping terms t_i. The hopping that appears in our equations will be a combination of these hopping terms that will be obtained considering only the kinetic term of the Hamiltonian as is done in the $U/t \to 0$ limit of the simple Hubbard Hamiltonian written in Eq. (14). The density of states $N(E_F)$ results from the given band dispersion, but as far as the instability conditions are concerned, all physical situations will range in between the two limits of homogeneous and nested bands we are considering. The influence of the specific dispersion of a system enters, therefore, our discussion through $N(E_F)$ and as we can see comparing Figs. 2(b) and 3(b), the geometry of a particular system will influence the physics qualitatively essentially in the region $U/t \leqslant 1$. In the $U/t > 1$ region, Figs. 2(b) and 3(b) display similar qualitative behavior and therefore the details of the considered system have no qualitative influence. However, in the case of sharp peaks in the density of states the instability conditions are easier to fulfill also in the $U/t \gg 1$ region. If we want the larger sensitivity of our physics to the doping δ, we must be in the rather strong-coupling regime $U/t > 1$ but also it is better that our density of states is rather flat since as we can see comparing Figs. 2(a) and 2(b), the larger δ slopes are reached in the homogeneous band case.

It is interesting to notice from Fig. 3(b) that the most unfavorable case for a Peierls stability is when $U/t \approx 1$, since the instability condition reaches a maximum at around $U/t \approx 1$ even at half-filling. The presence of a maximum is unavoidable at least at $\delta \to 0$ since in both the $U/t \to 0$ and $U/t \to \infty$ limits, the system is unstable at any electron-phonon coupling.

To illustrate that the choice of the c or ν parameters does not affect qualitatively our discussion, we display in Fig. 4 the U/t dependence of the instability condition for $\delta = 0.1$ shown in Fig. 3(b), for three different values of the exponent ν: $\nu = 3/2$ (full line), $\nu = 2$ also shown in Fig. 3(b) (dashed line) and $\nu = 4$ (short dashed line). We can see that there is no qualitative change and the maximum at $U/t \approx 1$ is just becoming a bit sharper as the crossover exponent ν grows. Finally, it is worth noting here also that the relations (23) and (24) can be straightforwardly generalized to the three-band Hubbard model, if we just replace in these relations t by $\tilde{t} = t_{pd}^2/(\varepsilon_p - \varepsilon_d)$.

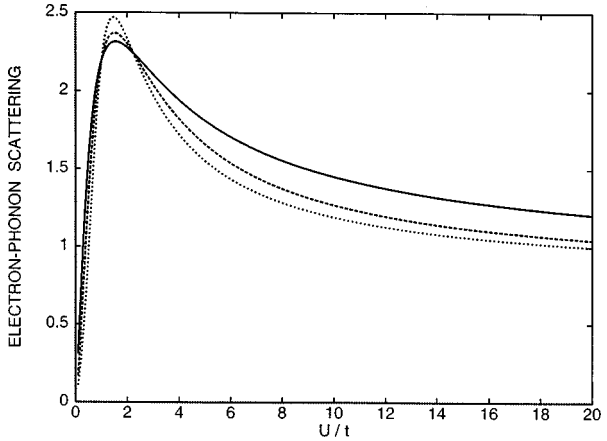

FIG. 4. The critical $\tilde{g}/t$ as a function of U/t when $N(E_F) \to \infty$, $\delta = 0.1$ and the same coefficients as in Figs. 2 except that ν takes three different values: $\nu = 3/2$ (full line), $\nu = 2$ (dashed line) also shown in dashed line in Fig. 3(b), and $\nu = 4$ (short dashed line).

V. FORWARD SCATTERING DOMINATES NEAR THE PS INSTABILITY

We have mentioned previously that in systems with short-range Coulomb repulsion like Hubbard models, phonon-driven PS instability is probable. Before the appearance of the instability, there are precursor effects that have unexpected implications on the phenomenology. When the system is close to the instability, the gradual appearance of the instability singularity changes qualitatively the scattering behavior of the system. This very particular regime of quasi-singular scattering will be shown to be potentially relevant for the understanding of various puzzles of the superconducting phenomenology of the oxides and could be intimately related to the high-T_c phenomenon.

The vicinity of the instability will affect the effective composite interaction $\Lambda(\mathbf{q}, \omega)$ given in Eq. (6). Up to now we studied the eventual divergence of Λ, next we will explore the effective interaction near the singularity. On the basis of our previous approach, we are able to obtain the dependence of the effective interaction on the Hubbard parameters. For simplicity we consider only dispersionless optical phonons and assume that the bare electron-phonon scattering amplitude has no relevant momentum structure. To obtain $\Lambda(\mathbf{q}, \omega)$ from Eq. (6), we need $V(\mathbf{q}, \omega)$ and $\Pi(\mathbf{q}, \omega)$. We will only consider static effects taking the $\omega \to 0$ limit.

In the RPA approximation we can replace the polarizability by the ''bare'' particle-hole bubble

$$\Pi_0(\mathbf{q}, \omega) = -2 \sum_{\mathbf{k}} \frac{f(\xi_{\mathbf{k}+\mathbf{q}/2}) - f(\xi_{\mathbf{k}-\mathbf{q}/2})}{\xi_{\mathbf{k}+\mathbf{q}/2} - \xi_{\mathbf{k}-\mathbf{q}/2} - \omega}, \qquad (25)$$

where $f(\xi_{\mathbf{k}})$ is the Fermi statistical factor and $\xi_{\mathbf{k}}$ the electronic dispersion. For example, in the oxides one can consider a next-nearest-neighbor tight-binding dispersion. In any case, the dispersion will not have qualitative influence on our discussion which is essentially generic. As for the Coulomb term V in Eq. (6), we use the interpolation formulas (15) and (20) to relate it to the Hubbard parameters. By calculating the bubble for a given dispersion using Eq. (25) we can, therefore, obtain $\Lambda(\mathbf{q}/\mathbf{k}_F, \tilde{g}/t, U/t, \delta)$. Our previous discussion for the divergence of Λ remains valid. Now, we exam-

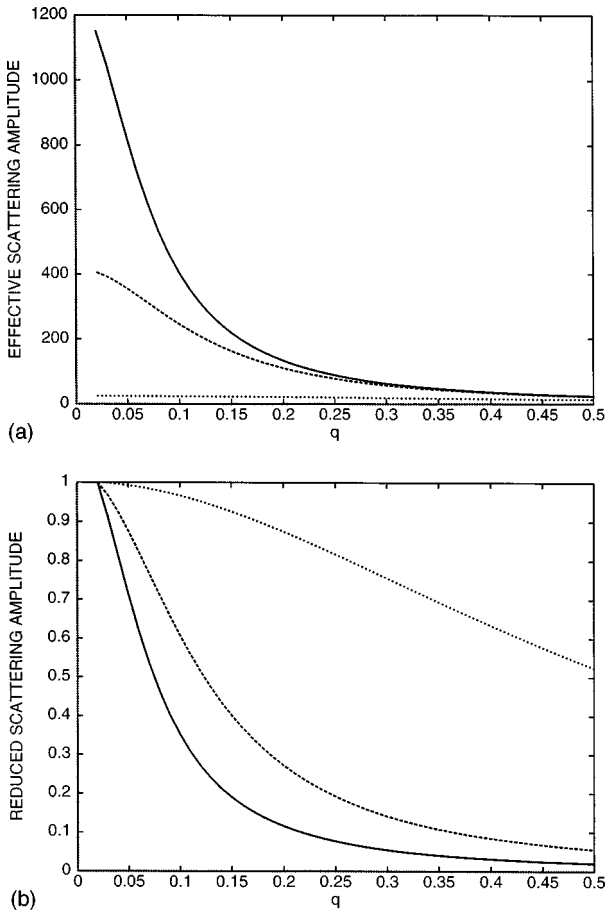

FIG. 5. (a) The phonon part of the absolute effective scattering amplitude $|\Lambda|$ as a function of $|q/2k_F|$ as we approach the instability reducing δ when $U/t=10$ (fixed) and $\tilde{g}/t=1$. Here we consider a next-nearest-neighbor dispersion as described in the text, and the evolution is given along the $(0,q)$ direction. (b) Same as in (a) reduced to unity. We see clearly the Lorentzian behavior of $\Lambda(q/2k_F)$ and the effective momentum cutoff that is the width of the Lorentzian.

ine Λ in the vicinity of the instability. Given $\tilde{g}/t$ and U/t we can investigate how the $\mathbf{q}/\mathbf{k}_F$ dependence of Λ correlates with δ.

We show in Fig. 5 the evolution of the momentum dependence of the absolute value of the effective composite interaction when we approach the instability. We focus here on the behavior of the phonon term neglecting the first term of Eq. (6) which is just a repulsive constant. For the results of Fig. 5 we consider a next-nearest-neighbor tight-binding dispersion in 2D: $\xi_{\mathbf{k}}=-2t[\cos(k_x)+\cos(k_y)]-4t'\cos(k_x)\cos(k_y)$ with $t=0.25$ eV, $t'/t=-0.45$ and $\mu=-0.44$ eV. This type of dispersion produces a van Hove peak in the density of states 10 meV below the Fermi level and is considered as a first approximation fit to LDA band-structure calculations for Y-Ba-Cu-O.[41] We take the Coulomb repulsion $U/t\approx 10$ fixed and we give to the phonon energies a value that could be relevant in the oxides $\Omega=40$ meV. The q dependence is along the direction $\mathbf{q}=(0,q)$ and in the interpolation formuli we use the coefficients b and μ obtained from the fit of Fig. 1, $c=1$ and $\nu=2$. We see in Fig. 5(a) that reducing δ we approach the instability that is signaled by a gradual appearance of a singularity in $\Lambda(q/2k_F)$ (here the instability occurs at $\delta^0\approx 0.1196$). The vicinity of the instability implies a strong enhancement of the effective composite interaction at forward scattering. This introduces a Lorentzian modulation in the q dependence of the effective scattering with a characteristic width (or smooth momentum cutoff) q_c that is becoming smaller as we approach closer to the instability [see Fig. 5(b)] and can get values as small as $k_F/10$. This momentum modulation will be shown to introduce qualitative changes on the phenomenology that could have some relevance in the oxides.

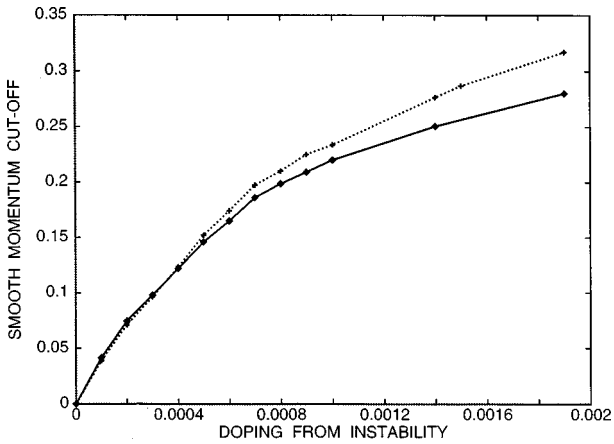

FIG. 6. The characteristic cutoff $q_c/2k_F$ or width of the Lorentzian as a function of $\delta-\delta^0$ where δ^0 is the hole concentration at which the phonon-driven instability occurs. The full line corresponds to the situation considered in Fig. 5, and the dashed line to the isotropic case where an homogeneous band is considered and the bubble is replaced by the Linhardt function for the same set of parameters.

Notice that a similar result has been reported recently using a slave-boson approach to a Hubbard model in the $U/t\rightarrow\infty$ regime with nearest- and next-nearest neighbors hopping and a Holstein electron-phonon coupling to a dispersionless phonon.[42] It is remarkable that our simple approach in the $U/t\rightarrow\infty$ regime provides results in surprisingly good agreement with those of Ref. 42. In particular, we obtain in this regime $\delta^0=0.1915$, while in Ref. 42 is reported $\delta^0=0.195$. Our approach gives the possibility to obtain analogous results at finite values of U/t. For example, in the case $U/t\approx 10$ considered in Fig. 5, the condition for instability is more difficult to fulfill than in the $U/t\rightarrow\infty$ regime, that is why it occurs at a smaller critical doping ($\delta^0\approx 0.1198$). In any case, the exact value of the Hubbard parameters is not physically relevant and we will restrict our discussion to relevant qualitative aspects.

The effective momentum cutoff or the characteristic width of the Lorentzian $\Lambda(q/2k_F)$ near the instability, will be a central parameter for our discussion that follows. In fact, we can reasonably fit the q dependence of $\Lambda(q/2k_F)$ with a Lorentzian of the form $\Lambda/(1+|q|^2/q_c^2)$, where q_c is the effective smooth cutoff of the interaction. We show in Fig. 6 the evolution of $q_c/2k_F$ as a function of the doping of holes from the instability $\delta-\delta^0$, where δ^0 is the critical hole concentration at which instability occurs. At small $\delta-\delta^0$, the behavior of $q_c/2k_F$ is generic, independent on the dispersion considered. In fact in Fig. 6 we consider two separate cases. The full line corresponds to the dispersion considered in Fig.

5 described in the previous paragraph. The dashed line corresponds to a simple isotropic case, where we do not calculate the bubble from Eq. (25) but just replace it by the Linhardt function considering also an homogeneous band where $N(E_F)=1/2W$ and in the interpolation formulas the same coefficients are taken. We remark that sufficiently close to the instability, the dependence of $q_c/2k_F$ on $\delta-\delta^0$ is the same in both cases. The momentum modulation of the effective scattering is, therefore, a robust effect that could be observed in different materials and characterizes the singularity in the effective composite interaction. Sufficiently close to the instability (for $q_c<k_F/4$) we have approximatively $q_c/2k_F\approx 220(\delta-\delta^0)$.

The extreme sensitivity of the momentum modulation of the effective interaction on the doping appears to be a serious handicap for the description of the doping behavior of the oxides within our simple approach. A similar sensitivity was also characteristic of the results of Ref. 42 to which our results fit in the $U/t\rightarrow\infty$ regime although very few points are reported there. It appears relevant for the oxides in the regime very close to the PS instability in which forward processes dominate the scattering. If this regime is confined in a very narrow range of doping then one might think that by doping the oxides we induce very small variations of the hole concentrations in the CuO_2 planes and we essentially built the charge reservoirs.[43] This has been an open issue up to now. Another possibility is that this pronounced δ sensitivity is an artifact of adiabatic mean-field considerations. In fact, using the correlated-random-field approximation and a conditional coherent-potential approximation[44,45] to study the ground-state phase diagram of a one-band Hubbard model without phonons, it was reported as numerical evidence for phase separation instability in an entire region of the phase diagram and not just on a line as in our case.[31] Unfortunately, for such types of treatment, a simple formalism like ours is not yet available, it is however plausible that nonadiabaticity will somehow broaden the transition lines even in our phase diagram. It is also conceivable that the system could be driven close to the PS instability from the Coulomb effects alone. In that case we also expect its effective scattering amplitude with phonons (or with some other bosonic field) to be enhanced at small momenta and the following discussion is still valid. This very interesting, delicate, and complex issue of the doping behavior will be the focus of our future investigations. In this manuscript, we attempt to establish the relevance of the vicinity to the PS regime for the understanding of the superconducting phenomenology of the oxides.

Similar plots to those of Fig. 6 can be made taking δ fixed and varying U/t. The approach to the instability has always the same qualitative effect of a strong enhancement of forward scattering processes.

VI. DOMINANT FORWARD SCATTERING IMPLIES MOMENTUM DECOUPLING IN SUPERCONDUCTIVITY

When forward scattering is dominant, there is ''momentum decoupling'' (MD) in the superconducting state, implying a different coupling in different regions of the Fermi surface. In the case of MD, the coupling at each region of the Fermi surface is proportional to the angularly resolved electronic density of states (ARDOS) at that region $N(E_F,\mathbf{k})=|v_F(\mathbf{k})|^{-1}$, and therefore *the anisotropies in the superconducting state are induced by the anisotropies of the density of states in the normal state*.

Let us now illustrate how MD appears for small momentum transfer processes and why it is the *only* situation which leads to ARDOS-dependent anisotropies in the superconducting state. The anisotropic Eliashberg equation in the off-diagonal sector, for an Einstein spectrum can be written as follows:

$$\Delta(\mathbf{k},i\omega_n)Z(\mathbf{k},i\omega_n) = \pi T\sum_m \int_{S_F}\frac{d^2p}{S_F}N(E_F,p) \times\frac{|g(\mathbf{k}-\mathbf{p})|^2\Omega}{\Omega^2+(\omega_n-\omega_m)^2}\frac{\Delta(\mathbf{p},i\omega_m)}{\sqrt{\omega_m^2+\Delta^2(\mathbf{p},i\omega_m)}}. \tag{26}$$

We assume here that all relevant scattering is done on the Fermi surface. Although we will consider small-q scattering, we suppose that its momentum range is, nevertheless, sufficiently larger than the k-level spacing and therefore, a density of states on the Fermi level $N(E_F,p)$ can be defined. The $\mathbf{k}$ dependence is contained in the coupling structure $|g(\mathbf{k}-\mathbf{p})|^2$.

In conventional s-wave superconductors, it is assumed that the interaction $|g(\mathbf{k}-\mathbf{p})|^2$ is smoothly varying on electronic energetic scales and it is almost constant on the Fermi surface. Then, one can obtain an isotropic $\mathbf{k}$-independent gap function and this is the classical scenario for an s-wave superconductor. Notice that, as will be clear later from the numerical calculations, even if the electronic ARDOS $N(E_F,p)$ is very anisotropic, we obtain isotropic gap from momentum-independent isotropic interaction.

On the other hand, if one assumes that $|g(\mathbf{k}-\mathbf{k}')|^2$ has a relevant momentum dependence in the vicinity of the Fermi surface (as is the case in a conventional d-wave scenario where this function reflects electron-spin fluctuation coupling) then we obtain a $\mathbf{k}$-dependent coupling and using Eq. (1) one can obtain an anisotropic gap. In that case, the anisotropy of the superconducting parameters is mainly imposed by the anisotropy of the interaction that we introduce and *not* from the anisotropy of ARDOS. This is considered in general as the only way to obtain strong anisotropies in the order parameter. According to the prevailing view, a strongly anisotropic order parameter reflects strongly anisotropic ''unconventional'' scattering (electron-phonon scattering is supposed to be rather isotropic).

However, it is possible to obtain significant ARDOS-induced anisotropies by considering an *isotropic electron-phonon interaction* dominated by forward-scattering processes. This can be illustrated taking an interaction which is sharply peaked at zero momentum $|g(\mathbf{k}-\mathbf{k}')|^2\approx g^2\delta(\mathbf{k}-\mathbf{k}')$. Then from Eq. (1), it is easy to see that there is *momentum decoupling*. We obtain a *momentum-independent* Eliashberg equation which provides the gap function $\Delta(\mathbf{k},i\omega_n)$ for each point $\mathbf{k}$ on the Fermi surface: $\Delta(\mathbf{k},i\omega_n)Z(\mathbf{k},i\omega_n)\approx N(E_F,\mathbf{k})\times$*isotropic terms*. This last

equation is analogous to the isotropic Eliashberg equation *with a coupling strength proportional to the value of the density of states at the given point of the Fermi surface* $N(E_F,\mathbf{k})$. The equations we obtain are isotropic with couplings that may be different in different regions of the Fermi surface depending on $N(E_F,\mathbf{k})$. Of course, the gap will be larger when the ARDOS and the resulting coupling are larger.

Since the coupling strength at each point k is proportional to the electronic ARDOS at that point and since the Eliashberg equations for the different points k are totally decoupled, the resulting momentum dependence of the gap will follow the momentum dependence of the ARDOS. We have, therefore, ARDOS-driven anisotropies. Notice also that small-q scattering is the *only* way to ARDOS-driven anisotropies. In fact, the ARDOS $N(E_F,\mathbf{k})$ is in a convolution integral with the interaction $|g(\mathbf{k}-\mathbf{k}')|$, and it is a well-known result of functional analysis that the δ function is the *unique* unity element of the convolution product.

Notice that a δ-function peak at $q=0$ is a rather unrealistic coupling function. We also noticed previously that we assume that the momentum range is large enough to allow the definition of the electronic ARDOS. However, MD occurs even for finite q provided q *is small compared to the characteristic momentum of the ARDOS variations over the Brillouin zone*. To illustrate this point we performed numerical calculations on a realistic two-dimensional BCS model. In that case the gap is given by

$$\Delta(\mathbf{k})=-\sum_{\mathbf{p},|\xi_p|<\Omega_D}\frac{\Lambda(\mathbf{k}-\mathbf{p})\Delta(\mathbf{p})}{2\sqrt{\xi_{\mathbf{p}}^2+\Delta^2(\mathbf{p})}}\tanh\left(\frac{\sqrt{\xi_{\mathbf{p}}^2+\Delta^2(\mathbf{p})}}{2T}\right). \tag{27}$$

We consider an isotropic s-wave electron-phonon coupling having at small momenta a Lorentzian behavior as a function of the norm of the exchanged momentum (our analysis concerns processes in which the momenta exchanged are small compared to the Fermi wave vector)

$$\Lambda(\mathbf{k}-\mathbf{p})=-\Lambda^0\left(1+\frac{|\mathbf{k}-\mathbf{p}|^2}{q_c^2}\right)^{-1}. \tag{28}$$

In this spectrum the electron-phonon scattering is dominated by the processes which transfer a momentum smaller than q_c. As we discussed earlier a scattering of the form of Eq. (28) describes well the effective pairing interaction when the electronic system is close to the phase separation instability. The closer the system is to the instability the smaller is q_c. Notice that the discussion that follows is unaffected by the use of another functional type of momentum cutoff, the relevant parameter being in fact q_c.

For clarity, we will consider here the simple nearest-neighbor tight-binding dispersion at half-filling $\xi_{\mathbf{k}}=-2t[\cos(k_x)+\cos(k_y)]$ (the lattice spacing is taken equal to unity). The Fermi surface is a square defined by $k_x=k_y\pm\pi$ and $k_x=-k_y\pm\pi$ with saddle points at $(0,\pm\pi)$ and $(\pm\pi,0)$. The minimum of the density of states on the Fermi surface is obtained at the points $(\pm\pi/2,\pm\pi/2)$ and therefore the characteristic length of the ARDOS variations over the Brillouin zone is $\pi/\sqrt{2}$. We expect, therefore, that for $q_c>\pi/\sqrt{2}$ the gap might be isotropic, while for q_c sufficiently smaller than $\pi/\sqrt{2}$, MD should prevail leading to ARDOS-induced anisotropies.

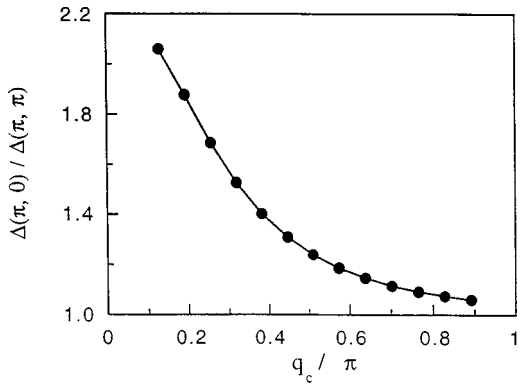

FIG. 7. Evolution of the anisotropy ratio as a function of the characteristic range of the exchanged momenta q_c. For $q_c<\pi/\sqrt{2}$ it increases sharply indicating the onset of MD.

This is precisely what is obtained numerically. We plot in Fig. 7 the ratio of the gap at $(0,\pi)$ over the gap at the points where the ARDOS is minimal $(\pi/2,\pi/2)$ as a function of q_c. We can see that for $q_c<\pi/\sqrt{2}$ this ratio begins to be appreciably different from unity indicating the onset of ARDOS-induced anisotropy because of MD. It is clear that for finite transferred momenta it is possible to obtain significant ARDOS-induced anisotropies. We also remark in Fig. 7 that even though the electronic ARDOS that corresponds to our dispersion is very anisotropic, the gap is isotropic when the range of the exchanged momenta is of the order k_F. In fact, when $q_c\approx\pi$ we have $\Delta(0,\pi)/\Delta(\pi/2,\pi/2)\approx 1$. Only if the k range of the interaction is sufficiently small we can have ARDOS-driven anisotropies in the order parameter no matter how anisotropic is the electronic system. This is why very different conventional superconducting materials with different electronic structures have an isotropic gap as observed for example by tunneling.

Therefore, the proximity of PS instability, manifests by the dominance of forward scattering that implies MD and *opens a new channel for anisotropic superconducting behavior even if the involved scattering is isotropic*. A central issue in our understanding of the mechanism of high-T_c is to establish whether the anisotropies in superconductivity are due to MD or are simply due to the more ''conventional'' channel of anisotropic scattering. For example, the approach of spin-fluctuation scattering in the analysis of d-wave superconductivity belongs to the second category.[46] In the following we will discuss some specific qualitative characteristics of MD that may help answer the crucial question of the origin of anisotropies in the oxides. We will see in particular that some puzzling qualitative aspects of the phenomenology of the oxides appear to be natural consequences of MD.

VII. MOMENTUM DECOUPLING AND THE SUPERCONDUCTING PHENOMENOLOGY OF THE OXIDES

We will focus on the superconducting phenomenology because obviously our approach neglects various aspects of the physics of the oxides. For example, magnetic effects are

not taken into account. In the normal-state phenomenology all these relevant parts of the physics manifest. However, in the superconducting state, the physics is dominated by the scattering with the bosonic processes that mediate the pairing (in conventional cases these bosons are phonons) and therefore our simple approach could be satisfactory if these processes are in the MD regime.

A. Marginality of the superconducting gap symmetry

The symmetry of the order parameter is in the center of the debate for the origin of high-T_c superconductivity. It is generally believed that the symmetry of the gap should also indicate the nature of the pairing mechanism. According to the general approach the symmetry should allow one to determine whether cuprates are conventional s-wave superconductors with an interaction that could be mediated by phonons, or whether they are unconventional d-wave superconductors in which case the pairing interaction should be due to spin fluctuations or to some other exotic mechanism. In the spirit of this approach, all high-T_c materials should have the same gap symmetry and their high critical temperatures should be intimately related to the symmetry of the gap.

The experimental situation is far from being in convincing agreement with the previous approach. Angle-resolved photoemission (ARPES) on overdoped Bi-Sr-Ca-Cu-O (Ref. 47) indicate an anisotropic s-wave gap having T-dependent anisotropy that will be shown later to be evidence in support of MD.[48] However, various phase sensitive[49] and node sensitive[50] experiments on $YBa_2Cu_3O_7$ report evidence of a sign reversal of the order parameter supporting d waves,[51] even though experimental contradictions still persist for Y-Ba-Cu-O (Refs. 52, 53) that will be shown later to be understood within MD as resulting from the orthorhombic distortion of the CuO_2 planes. On the other hand, it appears now established that electron-doped oxides are rather isotropic s-wave superconductors.[53]

Recent angle-resolvent photoemission results are very puzzling reporting that optimally doped $Bi_2Sr_2CaCu_2O_8$ has a node in the (1,1) direction consistently with d waves and in agreement with other measurements,[54–56] while on the other hand, the overdoped material has a finite gap in this same direction indicating anisotropic s-wave symmetry.[57] These last results indicate that the gap symmetry varies with the doping, yet the material remains a high-T_c superconductor (the overdoped material has $T_c=83$ K, while the optimally doped $T_c=92$ K). Recent Raman spectroscopy results confirm this behavior in Bi-Sr-Ca-Cu-O and report the same phenomenon of doping-induced gap symmetry transition in overdoped $Tl_2Ba_2CuO_{6+\delta}$.[58] High-T_c appears therefore *not associated with a specific gap symmetry, but rather associated with a ''volatility'' of the gap symmetry*. Such ''unconventional'' behavior is a smoking gun for momentum decoupling.

We will show in fact that, isotropic s-wave interaction (that could be mediated by phonons) in the momentum decoupling regime can lead to *either* s-wave or d-wave superconductivity depending on parameters that are *marginal* for the pairing. These parameters are the magnitude of the Coulomb pseudopotential μ^* and the characteristic momenta of the variations of the Coulomb pseudopotential μ^* compared to the characteristic momenta exchanged during the pairing interaction. It is possible that overdoped $Bi_2Sr_2CaCu_2O_8$ is (ARDOS-driven anisotropic) s-wave and $YBa_2Cu_3O_7$ as well as optimally doped $Bi_2Sr_2CaCu_2O_8$ are (ARDOS-driven anisotropic) d-wave superconductors all having *the same* attractive isotropic s-wave pairing interaction in the momentum decoupling regime. In addition, we report the possibility for transitions from s wave to d wave and vice versa by doping since μ^* depends sensitively on it, and this appears to be the case in Bi-Sr-Ca-Cu-O. Of course it will be obvious that *d-wave gap symmetry does not imply a spin-fluctuation pairing mechanism*.

Irrelevance of the symmetry of the order parameter for the free energy has also been reported in a model proposed to describe the ''spin gap'' in underdoped cuprates.[59] This property is also seen in another model in which the Fermi surface is divided in three independent pieces and the interaction has a low-energy cutoff.[60] The possibility for material specific gap is reported on a t-J model with three lattice

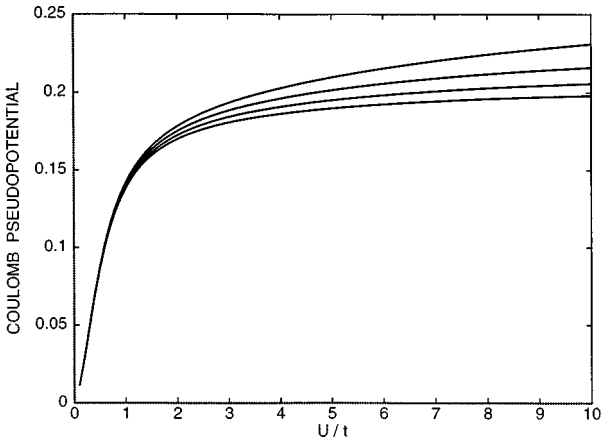

FIG. 8. The Coulomb pseudopotential given from Eq. (30) as function of U/t for different hole concentrations (from top to bottom $\delta=0,0.1,0.2,0.3$).

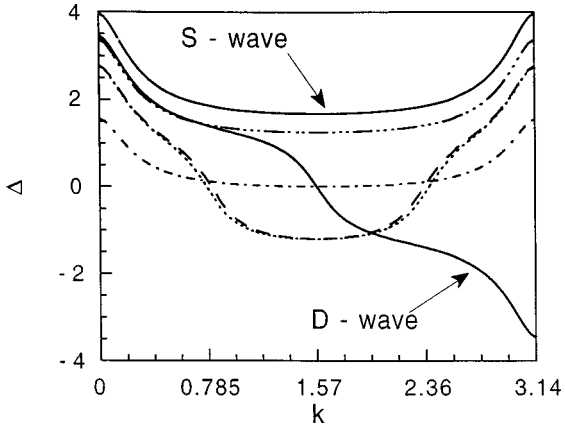

FIG. 9. The gap along a quadrant of the Fermi surface defined by $k_x+k_y=\pi$ as a function of k_x (or k_y) for a momentum-independent repulsion μ^* and Q_c(e-ph)$=\pi/12$. We consider the s-wave channel and $\mu^*=0$ (upper full line), $\mu^*/g^2=0.05$ (triple-dot-dashed line), $\mu^*/g^2=0.21$ (dot-dashed line), $\mu^*/g^2=0.22$ (dotted line), $\mu^*/g^2=0.30$ (dashed line), and the d-wave channel for the same μ^*/g^2 ratios (lower full line). The d-wave solution is independent of μ^*.

terms,[61] and similar numerical results were reported by Hellberg and Manousakis.[62] Nazarenko and Dagotto[63] proposed a specific Holstein model with nearest-neighbor attraction which leads to d-wave superconductivity with the spin fluctuations playing a secondary role. A similar approach was also developed by Song and Annett,[64] Kamimura *et al.*,[65] and Perali *et al.*[66]

Within our approach, μ^* corresponds to the first term of Eq. (6) renormalized by retardation. While our scheme accounts for the qualitative fact of the presence of μ^*, its quantitative evaluation is out of the question within our approach. Not only is a simple RPA approach questionable for the dynamic behavior, but the retardation renormalization itself in an anisotropic system is a very complex issue and obtaining quantitative results of that type is beyond the scope of this manuscript. We can, however, easily obtain some qualitative understanding of the behavior of μ^* in a Hubbard-type Fermi liquid (HFL) by considering a simplified picture of a material with homogeneous band and adopting that μ^* is given by the following relation:[67,68]

$$\mu^* = \frac{N(E_F)V}{1 - N(E_F)V \ln(\Omega/W)}. \tag{29}$$

The renormalization of the Coulomb repulsion by retardation is explicit. In fact there is a characteristic ''distance'' between electrons in the superconducting state associated with the characteristic time for the absorption of the virtual phonon that mediates the pairing. Since Eq. (29) is valid in the case of homogeneous bands we have $2N(E_F) \approx W^{-1}$. Then combining with Eqs. (15) and (20) we obtain

$$\mu^* = \frac{1}{2}\left[1 + \frac{1}{1 + c(U/t)^{\nu}}\left(\frac{U/t}{2z\delta + 2(1-\delta)/[1 + b(U/t)^{\mu}]} - 1\right)\right]\left\{1 - \frac{1}{2}\left[1 + \frac{1}{1 + c(U/t)^{\nu}}\left(\frac{U/t}{8\delta + 8(1-\delta)/[1 + b(U/t)^{\mu}]} - 1\right)\right] \times \ln\left[\frac{\Omega}{t}\left(\frac{1}{8\delta + 8(1-\delta)/[1 + b(U/t)^{\mu}]}\right)\right]\right\}^{-1}. \tag{30}$$

We show in Fig. 8 the U/t dependence of μ^* for different hole concentrations δ. When $U/t \leq 1$ the doping is irrelevant, while in the $U/t > 1$ regime it becomes relevant. The larger the hole concentration δ, the smaller the sensitivity of μ^* on the local Coulomb repulsion U/t in the $U > t$ region. Usually, in conventional superconductors, μ^* plays just the role of an effective negative coupling,[17] but for a system in the MD regime μ^* becomes a crucial parameter having unexpected implications on the gap symmetry.

We performed calculations on a BCS model as that in Eq. (27), but the interaction is taken here $\tilde{\Lambda}(\mathbf{q}) = \Lambda(\mathbf{q}) + \mu^*(\mathbf{q})$. The effective interaction is, therefore, the sum of the attractive interaction, due to the electron-phonon coupling Λ, that will be taken to have a form as that in Eq. (28), and the effective Coulomb repulsion $\mu^*(\mathbf{q})$. The pairing scattering is dominated by the processes which transfer a momentum smaller than the effective momentum cutoff defined here as $Q_c^{\text{e-ph}}$. $Q_c^{\text{e-ph}}$ is the relevant parameter and the particular shape of the interaction is irrelevant. As for the repulsive interaction, it is first supposed momentum independent $\mu^*(\mathbf{q}) = \mu_0^*$ as in Eq. (30) (hard-core-like yet finite repulsion or contact repulsion). Band-structure effects are marginal for our discussion and for clarity we show, here also, results corresponding to the simple nearest-neighbor tight-binding dispersion at half-filling $\xi_{\mathbf{k}} = -2t[\cos(k_x) + \cos(k_y)]$ (the lattice constant is taken equal to unity).

We show in Fig. 9 some of the calculated momentum-dependent gap functions on the Fermi surface, for different values of μ_0^* in both the d-wave and s-wave channel. When k (k_x or k_y) varies from 0 to π we cover a quadrant of the Fermi surface which is defined by $k_x + k_y = \pi$. Here we take $Q_c^{\text{e-ph}} \approx \pi/12$ which places us deeply in the momentum decoupling regime and might characterize a system rather close to the phase separation instability (for example $\delta - \delta^0 \approx 10^{-4}$). The momentum dependence of the gap in the s-wave channel at zero repulsion (upper full line) is due to momentum decoupling. The anisotropy in both channels is therefore ARDOS driven since our interaction is isotropic.

When we introduce μ^* in the s-wave channel, the gap is reduced by a constant amount in all directions (triple-dot-dashed line) resulting therefore in an effective enhancement of the anisotropy. At a critical value of the repulsion which in the case considered in Fig. 9 is on the order $\mu^*/g^2 \approx 0.21$ (dot-dashed line), the gap becomes almost zero in the (π,π) direction, and we have a *discontinuous* transition to a new gap symmetry structure with two nodes in the quadrant shown in Fig. 9 (dotted and dashed lines). In this new state the gap becomes *independent* of the magnitude of μ^* and the areas of the Fermi surface in which the gap is positive are equal to the areas in which the gap is negative. We will see next that this new state is not the physical state occupied by the system because at these μ^* the d-wave solution is energetically more favorable.

The d-wave solution is also characterized by the independence of the gap on the magnitude of μ^*. The origin of the repulsion-independent gap lies on the momentum independence of μ^*, and on the equality of the Fermi-surface areas with positive and negative gap. We can see this analytically by considering a circular Fermi surface. If the gap on the Fermi surface has the form $\Delta_{\mathbf{k}} = \Delta\cos(n\phi)$ where n is the number of nodes and ϕ is the polar angle in the usual polar coordinates, then the momentum-independent repulsive contribution to the gap function becomes proportional to the integral

$$I = \int_0^{2\pi} d\phi \, \frac{\Delta\cos(n\phi)}{\sqrt{\xi_{|\mathbf{k}|}^2 + \Delta^2\cos^2(n\phi)}} = 0, \tag{31}$$

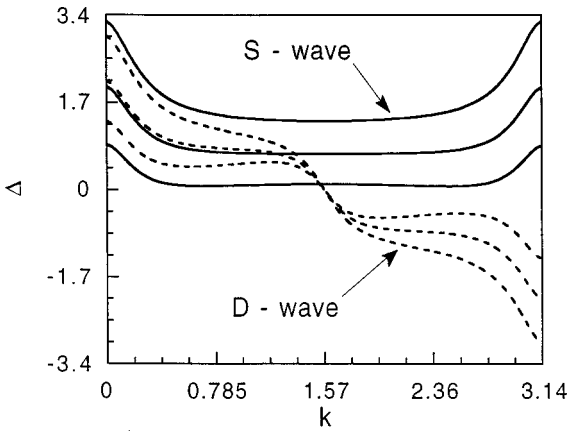

FIG. 10. The s-wave gap (full lines) and the d-wave gap (dashed lines) as a function of k_x (or k_y) on a quadrant of the Fermi surface, for three different values of the repulsion $\mu_0^*/g^2=0.05$, 0.15, and 0.25, in the case $Q_c(\text{e-ph})=\pi/12$ and $Q_c(Cb)=\pi/4$. The smaller the ratio μ_0^*/g^2 the larger is the absolute value of the gap in both the s- and d-wave solutions.

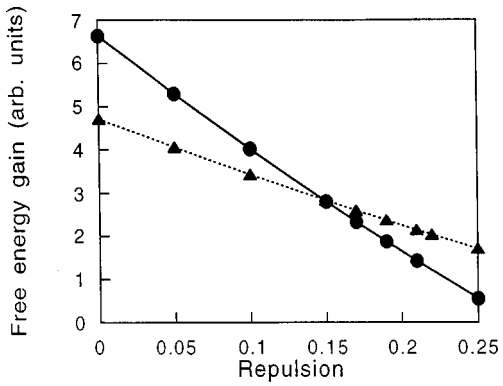

FIG. 11. The absolute value of the free energy gain due to the superconducting transition as a function of the ratio μ_0^*/g^2 for $Q_c(\text{e-ph})=\pi/12$ and $Q_c(Cb)=\pi/4$. The dotted line (triangles) corresponds to the d-wave solution and the full line (circles) to the s-wave solution. The physical solution is that with the higher absolute free-energy gain (lower free energy).

which is *identically* zero. Therefore, a gap changing sign periodically on the Fermi surface eliminates the effect of any *momentum-independent* repulsion providing a qualitative understanding of the discontinuous nature of the transition in the s-wave channel in Fig. 9 (from dot-dashed line at $\mu^*/g^2=0.21$ to dashed line at $\mu^*/g^2=0.22$). We remark that the nodes we obtain have a finite slope and therefore a linear T dependence of the penetration depth in the $T\rightarrow 0$ regime is plausible.

The q independence of μ^* in the simple case considered in Eq. (30) is due to the locality of the repulsion in our model. However, in realistic situations μ^* is expected to be momentum dependent. This momentum dependence can be either due to a nonlocal repulsion or due to the retardation renormalization of this quantity since it is always associated with a characteristic time a characteristic distance in a Fermi liquid. For example, if the diameter of the pairs in the oxides is about four times the lattice spacing, we could expect a characteristic momentum of the order $k_F/4$. A realistic calculation of the q dependence of μ^* in the oxides would require a retarded framework which is very complicated for a Hubbard model and is in any case beyond the scope of this manuscript.

To introduce a smooth momentum cutoff for the variations of μ^* and be more realistic, we consider a structure analogous to that of the pairing interaction written at small q as $\mu^*(\mathbf{q})=\mu_0^*[1+|\mathbf{q}|^2/(Q_c^{Cb})^2]^{-1}$, in which case Q_c^{Cb} represents the characteristic range of the exchanged momenta (smooth cutoff) in the repulsive interaction. The important parameter is the momentum cutoff in the repulsive interaction Q_c^{Cb} compared to that in the attractive pairing interaction $Q_c^{\text{e-ph}}$. We show in Fig. 10 the s-wave and d-wave gap solutions for $Q_c^{Cb}=\pi/4$ and $Q_c^{\text{e-ph}}=\pi/12$. Now the d-wave solution is not μ^* independent but it still appears to be less sensitive to μ^* than the s-wave solution. It is clear from Fig. 10 (and also Fig. 9) that at some critical μ^* the absolute d-wave gap will become larger in average than the s-wave gap, and this will become the energetically favorable state.

To find out which one between the s-wave and d-wave solutions is the physical state of the system, one has to calculate the free-energy gain due to the superconducting transition,[69] the physical solution being that with the higher absolute free-energy gain (the lower free energy). Of course, the solution with the higher free-energy gain is that for which the integral of the absolute value of the gap on the Fermi surface is higher and this is also the solution with the higher T_c. The condensation free energy at zero temperature is given by[70]

$$F\approx\frac{1}{N}\sum_{\mathbf{k}}\left\{\xi_{\mathbf{k}}\frac{\sqrt{\xi_{\mathbf{k}}^2+\Delta_{\mathbf{k}}^2}-\xi_{\mathbf{k}}}{\sqrt{\xi_{\mathbf{k}}^2+\Delta_{\mathbf{k}}^2}}-\frac{\Delta_{\mathbf{k}}^2}{2\sqrt{\xi_{\mathbf{k}}^2+\Delta_{\mathbf{k}}^2}}\right\}. \qquad (32)$$

In Fig. 11, we show the evolution of the free-energy gain (absolute value of the free energy due to the superconducting transition in arbitrary units) as a function of μ_0^*/g^2 in the case $Q_c^{Cb}=\pi/4$ and $Q_c^{\text{e-ph}}=\pi/12$. The s-wave solution is favorable when μ_0^*/g^2 is small but when this ratio takes values larger than a critical value of the order of $\mu_0^*/g^2\approx 0.15$ then the d-wave solution becomes more favorable. Therefore, transitions from s-wave to d-wave superconductivity and vice versa appear possible depending on details. Notice also that the evolution of T_c follows essentially that of the free-energy gain, and from Figs. 10 and 11 one can conclude that *the negative effect of μ^* on T_c is smaller in the case of d waves than in the case of s waves*.

Such s-d transitions occur in our system at conventional values of the Coulomb pseudopotential already observed in low-T_c superconductors.[67] The critical μ_0^* is very dependent on the ratio $Q_c^{\text{e-ph}}/Q_c^{Cb}$. We studied the evolution of the free-energy gain in the s- and d-wave channels as a function of μ_0^*/g^2 for different values of $Q_c^{\text{e-ph}}/Q_c^{Cb}$. This allowed us to construct the phase diagram shown in Fig. 12. We also made an analogous study in the case of different momentum structures of μ^* having an effective momentum cutoff and the resulting phase diagrams are similar to that of Fig. 12. When for a given $Q_c^{\text{e-ph}}/Q_c^{Cb}$ the ratio μ^*/g^2 is larger than the critical value shown in Fig. 12, the gap is d wave. It is clear that the smaller the ratio $Q_c^{\text{e-ph}}/Q_c^{Cb}$, the smaller is the value of the critical repulsion, while for $Q_c^{\text{e-ph}}$ of the same order as

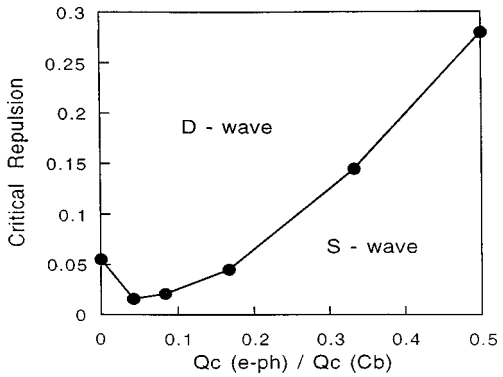

FIG. 12. Phase diagram. The critical repulsion μ_0^*/g^2 for the transition from s-wave to d-wave superconductivity as a function of the ratio $Q_c(\text{e-ph})/Q_c(Cb)$. The upper region of the graph corresponds to the d-wave state.

Q_c^{Cb} the d-wave solution is impossible and this is probably the case in low-T_c metallic superconductors. Since in the MD regime $Q_c^{\text{e-ph}} \ll k_F$, we can also have $Q_c^{\text{e-ph}} \ll Q_c^{Cb}$, in which case s- and d-wave superconductivity are energetically close and both states are physically acceptable depending on details like the precise value and structure of μ^*.

It is quite plausible that by overdoping Bi-Sr-Ca-Cu-O we induce a transition from d-wave to s-wave gap as reported by Kelley *et al.*[57] While a realistic calculation of μ^* in Bi-Sr-Ca-Cu-O is not possible within our simple approach, there are qualitative points from our analysis that make plausible this d-s transition by overdoping Bi-Sr-Ca-Cu-O. In fact, the smaller the hole doping δ, the smaller is expected to be the effective cutoff of the pairing interaction (see Fig. 5) and therefore the d state is favored. As we enhance δ, we move gradually away from the instability enhancing $Q_c^{\text{e-ph}}/Q_c^{Cb}$ (see Fig. 5) favoring therefore a transition to s wave (see Fig. 11). In addition, the anisotropic s-wave state is obtained naturally in the overdoped regime [as far as possible from the antiferromagnetic (AF) state], since the closer we are to the AF regime, the larger is expected the ratio μ^*/g which favors the d state within our analysis. On the other hand, if the anisotropies were imposed by anisotropic scattering for example, with spin fluctuations, such variation of the gap symmetry with doping appears very difficult to understand.[46]

It is important to notice that the d-wave state we obtain is anisotropic and its anisotropies are driven by the ARDOS anisotropies in the same way as for the s-wave state discussed in the previous section.[48] This is clear in Figs. 9 and 10, where the d-wave solution away from the $(\pi/2,\pi/2)$ direction has exactly the form of the s-wave solution. When we are in the MD regime we always have different couplings in different regions of the Fermi surface whatever the symmetry of the gap. In particular all of our discussion that follows on the origin of the dip structure, the correlation of gap, dip, and DOS anisotropies, and the asymmetry of superconductor–insulator–normal-metal (SIN) tunnel spectra[48] is independent of the gap symmetry. Notice finally that many of the contradictions in the gap-symmetry spectroscopic experiments on $YBa_2Cu_3O_7$ may be quantitatively understood within our picture if we include the orthorhombic distortion of the CuO_2 planes (this will be discussed later). We should only notice here that the orthorhombic distortion turns out to be favorable for the d channel and appears therefore natural that in Y-Ba-Cu-O the d channel is robust (in the d channel the d-wave component is dominant, however, because of the distortion there exists also a minor s component).

B. Temperature dependence of the shape of the anisotropy

Clearly, a fundamental issue in the analysis of the superconducting behavior of the oxides should be to distinguish whether the anisotropies or even the d symmetry reflect anisotropies of the scattering amplitude (like that with spin fluctuations) or are simply due to momentum decoupling. If the anisotropy is driven by anisotropic scattering, then it should be temperature independent since usually the scattering amplitude is also temperature independent. This is contradictory to the temperature dependence of the anisotropy in slightly overdoped $Bi_2Sr_2CaCu_2O_{8+\delta}$ reported in Ref. 47. According to Ref. 47, while the gap in the $\Gamma-M$ direction $(0,\pi)$ vanishes exactly at T_c, in the $\Gamma-X$ (π,π) direction a smaller critical temperature characterizes the gap variations. This has been analyzed in Ref. 71 as an indication of a mixed symmetry $s+d$ gap, assuming that the different gap symmetries have different T dependences near T_c. We will give an alternative interpretation of this behavior in the framework of MD.[48] Our basic observation is that the system behaves as if the superconductivity at $\Gamma-M$ direction is not influenced by the superconductivity at the $\Gamma-X$ direction, and this is precisely the implication of MD.

If MD was perfect in $Bi_2Sr_2CaCu_2O_{8+\delta}$, the temperature at which the gap disappears in the $\Gamma-X$ direction should be smaller than that in the $\Gamma-M$ direction. In fact, since the ARDOS is smaller in the $\Gamma-X$ direction the coupling is smaller and therefore T_c is naturally smaller. The critical temperature for superconductivity is the temperature at which not any gap is present in any direction, and therefore it corresponds to the temperature at which the larger gap (in the $\Gamma-M$ direction) reflecting the larger coupling (the larger ARDOS) vanishes. Therefore, if MD is perfect the anisotropy *diverges* in the vicinity of T_c since the gap away from the optimal direction is expected to vanish at a temperature smaller than T_c.

In the realistic situations where MD is not perfect, we do not expect a divergence but a strong enhancement of the anisotropy near T_c, which could very well account for the experimental results. We will show in the following how the results of Ref. 47 can be reproduced qualitatively when finite momenta are transferred, doing numerical calculations with the BCS model that we used previously [Eqs. (27) and (28)] and the same nearest-neighbor tight-binding dispersion. In Fig. 13, we report the temperature dependence of $\Delta(0,\pi)$ and $\Delta(\pi,\pi)$ (gaps at the $(0,\pi)$ and $(\pi/2,\ \pi/2)$ points of the Fermi surface, respectively) for different values of q_c, and in Fig. 14 we give the corresponding temperature dependence of the anisotropy ratio $R=\Delta(0,\pi)/\Delta(\pi,\pi)$. The critical temperatures are obtained solving numerically the Hermitian eigenvalue problem of the linearized BCS equations near T_c. It is remarkable that the T_c we obtain corresponds precisely to the temperature at which the larger gap [in the $(0,\pi)$ direction] vanishes. The momentum grid in these temperature-dependent solutions has to be adapted to the gap magnitude and for each one of the points, several hours of CPU time in

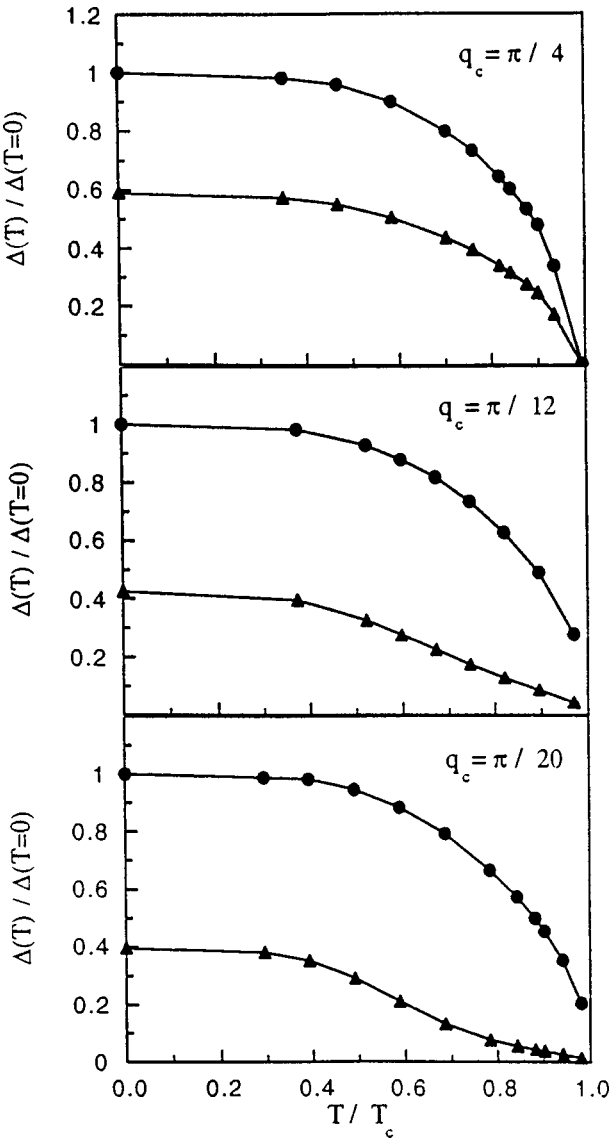

FIG. 13. Temperature dependence of the gap Δ in the $(\pi,0)$ (circles) and in the (π,π) (triangles) directions for three characteristic ranges of exchanged momenta q_c. Lowering q_c there is a continuous evolution in the (π,π) direction through perfect MD, implying two different critical temperatures.

a standard Unix workstation are necessary. The points very near T_c require a few days of CPU time. The regularity of our points reflects the quality of the numerical convergence, and the linear temperature behavior of the anisotropy ratio near T_c is an intrinsic characteristic.

When $q_c=\pi/4$ the DOS-induced anisotropy because of partial MD is already significant ($R\approx 1.7$), but the anisotropy is almost temperature independent. In fact one can see in Fig. 14 that the ratio R is temperature independent in that case. When we consider smaller values of q_c, there is a continuous deformation of the T dependence of $\Delta(\pi,\pi)$ from the large-q_c regime where the anisotropy ratio R is almost temperature independent towards the $q_c\rightarrow 0$ regime where as expected in perfect MD, $\Delta(\pi,\pi)$ should have a BCS behavior going to zero at a temperature on the order of $0.6T_c$, and therefore the anisotropy ratio should diverge close to T_c. We see this clearly in Fig. 14, where the anisotropy ratio R

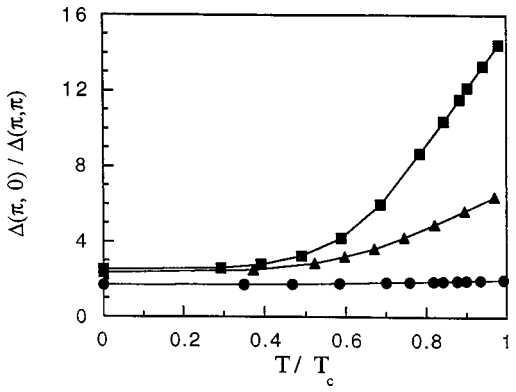

FIG. 14. Temperature dependence of the anisotropy ratio for $q_c=\pi/4$ (circles), $q_c=\pi/12$ (triangles), and $q_c=\pi/20$ (squares). The increase with temperature of this ratio is a clear indication of MD.

reaches values one order of magnitude larger near T_c. At a first view, the results of Ref. 47 indicate the perfect MD regime but one should bear in mind that if the small gap is smaller than the temperature at which it is measured, it is experimentally inaccessible.[72] Taking into account such thermal effects neglected in our BCS model, the results of Ref. 47 can be qualitatively understood even with q_c of the order $\pi/10$. A remarkable point in Fig. 14, is that the anisotropy ratio R grows linearly as we increase T towards T_c in the MD regime. We verified this result numerically but we have not succeeded in obtaining an analytic understanding of it.

If the anisotropy is due to an anisotropic interaction and does not reflect the DOS anisotropy, then we expect it to be *temperature independent*. We can understand this very easily by remarking that the same interaction that leads to the gap also leads to T_c (that is why the ratio $2\Delta/T_c$ has a physical meaning). If the gap anisotropy at $T\rightarrow 0$ reflects the anisotropy of the interaction, then since the same interaction is present at $T=T_c$, the same gap anisotropy should also be present when $T\rightarrow T_c$. This is also the result of numerical simulations in the spin-fluctuation pairing scenario. Therefore, *the enhancement of anisotropy with temperature is evidence of MD*, and cannot be understood in the case of anisotropic interactions like these considered in the spin-fluctuation pairing scenario.[46] The study of the T dependence of the shape of the anisotropy is therefore a crucial test for the pairing mechanism.

C. The behavior of the anomalous dip above the gap in the density of states

The presence of a characteristic dip structure above the gap in the density of states of all high-T_c materials is now established. Various interpretations of this dip have been proposed in the literature.[73–76] It has been shown in Refs. 74–76 that when the coupling strength exceeds some characteristic value of the order $\lambda\approx 2$ then the dip structure appears above the gap at an energy of the order 3Δ. This dip structure has nothing to do with the spectral structure of the phonons and its position in energy is correlated with the value of the gap and not with phonon energies. The dip is a lifetime effect of the pairs[75,77] and accompanies other characteristic qualitative modifications of the BCS phenomenol-

ogy at large couplings like, for example, the absence of a Hebel-Slichter peak[78–80] and the anomalous T dependence of the density of states of excitations.[75,76] Therefore, within conventional BCS theory, if the coupling is larger than $\lambda \approx 2$ [which corresponds to $2\Delta/T_c > 5.0$ (Refs. 16,17)] then the dip must be visible above the gap, and since experiments measure large gap ratios the dip is naturally present as discussed in Refs. 75 and 76. The following analysis of the anisotropic behavior of the dip structure could be considered as a strong support to the dip interpretation of Refs. 74–77.

The first remarkable point in the study of the density of states within strong-coupling BCS theory is that the isotropic strong-coupling solutions of Eliashberg equations provide a dip structure in surprisingly good agreement with experiment.[75,77] It is well known that the oxides are highly anisotropic and the relevance of isotropic Eliashberg calculations is very surprising. The answer to this puzzle is given by MD. In fact, as we have discussed in Sec. VI, in the case of MD we obtain momentum-independent Eliashberg equations in the different points of the Fermi surface. If MD were perfect, at each point of the Fermi surface the superconducting behavior would obey the isotropic Eliashberg equations with a coupling strength proportional to the ARDOS at that point. Within the analysis of the dip given in Refs. 75 and 76, the dip visibility is correlated with the magnitude of the coupling strength. The stronger the coupling, the sharper and deeper the dip, which can be viewed as *a qualitative measure of the coupling strength*. According to the dip interpretation of Refs. 75 and 76, an eventual anisotropy of the dip (reported for example by ARPES) should indicate *different couplings in different directions*.

Within the MD scenario, we expect in the case of Bi-Sr-Ca-Cu-O the coupling strength to be stronger in the $\Gamma - M(0,\pi)$ direction since the extended van Hove singularity is present there and the ARDOS is higher. We also expect that moving away from the $\Gamma - M(0,\pi)$ towards the $\Gamma - X$ (π,π) direction on the Fermi surface, the coupling strength should be strongly reduced. There is a qualitative feature common to *all* ARPES experiments that certifies that indeed moving from the $\Gamma - M$ to the $\Gamma - X$ direction on the Fermi surface *we move from a strong-coupling regime to a weak-coupling regime*. In fact in the $\Gamma - M$ direction is clearly seen a sharp dip structure above the gap that according to Refs. 75 and 76 indicates rather strong coupling $(\lambda \approx 3)$. It is a *common trend of all ARPES experiments* that moving from $\Gamma - M$ towards $\Gamma - X$, the visibility of the dip drops gradually and the dip is totally absent in the $\Gamma - X$ direction. We recall that not only the dip visibility drops but also the electronic ARDOS and the gap magnitude. To our analysis this might be considered as a strong support to MD. We are not aware of another theoretical interpretation for the *correlation of the dip anisotropy, with the ARDOS and gap anisotropies*.

In the scheme of MD, we can also understand a fundamental characteristic of the experimental measurements of the density of states in the oxides. In fact the tunneling[81] and ARPES measurements in the optimal for the gap direction[82] report very similar dip structures above the gap in the density of states of excitations. This is very surprising since ARPES reports the spectral function at some specific direction, while the tunneling spectrum arises from the contribution of all parts of the Fermi surface. But within the MD scheme, the tunnel spectrum is made up by quasi-independent contributions of the various parts of the Fermi surface. The contribution of the $\Gamma - M$ region naturally dominates, since the van Hove singularity is extended and covers around 30% of the Brillouin zone. The dip structure seen by tunneling reflects the contribution of the singular region and is therefore equally sharp with the dip structure seen by ARPES in this direction.[77]

Since the physics is dominated by the contribution of the singular regions, we can naturally understand the asymmetry of the tunneling spectra of Ref. 83. In fact, the dip structure is seen only at negative sample bias, because the Van Hove singularity in the $\Gamma - M$ $(0,\pi)$ direction is *below* the Fermi level. Measuring at positive sample bias, the dynamic behavior reflects the density of states above the Fermi level (as in inverse photoemission). The presence of the dip at negative sample bias and its absence at positive sample bias,[83] indicates that the density of states at an energy of the order of Δ (the optimal gap in the $\Gamma - M$ direction) above the Fermi level, is at least 30% smaller than that at an energy Δ below the Fermi level, and this can be easily obtained given the presence of the Van Hove singularity in the $\Gamma - M$ direction. Because the DOS is smaller above the Fermi surface, the coupling is smaller and the dip is no more visible.[75,77]

D. Large effects of orthorhombicity in Y-Ba-Cu-O without involving the chains

The symmetry of the order parameter in $YBa_2Cu_3O_7$ is still controversial. While phase-sensitive experiments established that the order parameter reverses its sign on the Fermi surface indicating d-wave symmetry, c-axis Josephson tunneling experiments on the same material indicated the existence of a significant s component.[84,85] This late conclusion seems to be reinforced by the relative insensitivity of the superconducting critical temperature on the presence of nonmagnetic impurities or defects.[86] It appears experimentally that the gap has a dominant d-wave component but also a significant s-wave component. It has been argued that this behavior indicates the existence of two different condensates.[87]

The mixing of s and d components arises naturally when the lattice is orthorhombically distorted.[88] Large orthorhombic distortions have therefore been invoked in order to understand the experimental reports in $YBa_2Cu_3O_7$.[89–91] However, the orthorhombic distortion of the CuO_2 planes in the case of $YBa_2Cu_3O_7$ is only a few percent $(\approx 3\%)$ and such a small distortion cannot induce significant mixing of s components in a d-wave spin-fluctuation-mediated pairing. In the case of $Bi_2Sr_2CaCu_2O_8$ such orthorhombic distortion is essentially absent and the in-plane structure is tetragonal.[92] The absence of mixing of gap symmetries in $Bi_2Sr_2CaCu_2O_8$ could indicate that the orthorhombic distortion in $YBa_2Cu_3O_7$ is indeed involved in the mechanism that leads to the symmetry mixing in this last material.

To reconcile the large orthorhombicity effects required by the phenomenology and spin-fluctuation-mediated pairing, Carbotte and collaborators argued that the Cu-O chains are involved in superconductivity and a large part of the condensate is located there.[91] Since the chain band concerns only

one direction in the *ab* plane, if chains are involved, large in plane anisotropies are reasonable. Large anisotropies between the *a* and *b* directions are also reported in microwave penetration depth measurements.[93] On the other hand, supposing that the chains contain part of the condensate and are therefore crucially involved in the pairing mechanism is difficult to reconcile with the fundamental similarities of superconductivity in Y-Ba-Cu-O with that of the other high-T_c cuprates where the chains are absent.[94] There are also arguments based on LDA calculations indicating that the chains not even contribute in the transport.[43] Whether the chains are involved in the pairing or not is not yet a definitely answered question, there are nevertheless strong arguments supporting that the interesting physics happens in the CuO_2 planes.[43,94] We stress here that if we are able to answer experimentally the question of the relevance of the chains, we could also give strong constraints on the origin of anisotropic superconductivity in YBCO.

The effect of orthorhombicity on the CuO_2 plane is to make inequivalent the *a* and *b* axes and in $YBa_2Cu_3O_7$ the difference in these lattice constants is less than $\approx 3.5\%$. For such small variations, to a first order, in a tight-binding dispersion the hopping along the two different axes will be inequivalent with differences of the same order. Therefore, to see the effect of the orthorhombic distortion in the CuO_2 planes we take in our dispersion relations the hopping terms along k_x and k_y inequivalent. For example, in the simpler next nearest-neighbors tight-binding fit to the LDA band-structure calculations for the CuO_2 planes of $YBa_2Cu_3O_7$ that we already considered in Sec. V,[41] we must write now $\xi_{\mathbf{k}} = -2t[\cos(k_x)+(1+\beta)\cos(k_y)]-4t'\cos(k_x)\cos(k_y)-\mu$ where β is the orthorhombicity factor of the order $\approx 4\%$ in Y-Ba-Cu-O and the other parameters are as explained in Sec. V. We can inject this dispersion in Eq. (27) and solve it to obtain the gap function $\Delta(\mathbf{k})$ for the orthorhombically distorted system. Making inequivalent the directions *a* and *b* in the band dispersion, we have inequivalent Fermi velocities and therefore we naturally expect in the MD regime different absolute values of the gap along *a* and *b*.

Indeed, taking $\mu^*/g \approx 0.075$ in Y-Ba-Cu-O we obtained very large differences in the gap along (near) *a* and *b* with very small realistic values of the distortion $\beta \approx 0.04$. The full line in Fig. 15(a) shows the evolution of the ratio Δ_a^2/Δ_b^2 as a function of the distortion factor β. We consider the energetically favorable *d*-wave channel and when we rotate 90° from *a* to *b* the gap changes sign being dominantly *d* wave. It must be noticed that such large ''distortions'' on the superconductive behavior are characteristic of MD and could be an element of answering the central question of whether anisotropies are driven by anisotropic scattering or by MD. We also consider for comparison the Millis, Monien, and Pines (MMP) phenomenological scattering with spin fluctuations[95] in the static limit

$$\Lambda \approx \frac{\Lambda_0}{1+\xi_M^2(\mathbf{q}-\mathbf{Q})^2}, \tag{33}$$

where $\mathbf{Q}=(\pi,\pi)$, the coherence range of the antiferromagnetic spin fluctuations ξ_M is taken on the order of three lattice spacings as in the experiment[95] and Coulomb pseudopotential is neglected. We show in Fig. 15(a) with dashed line

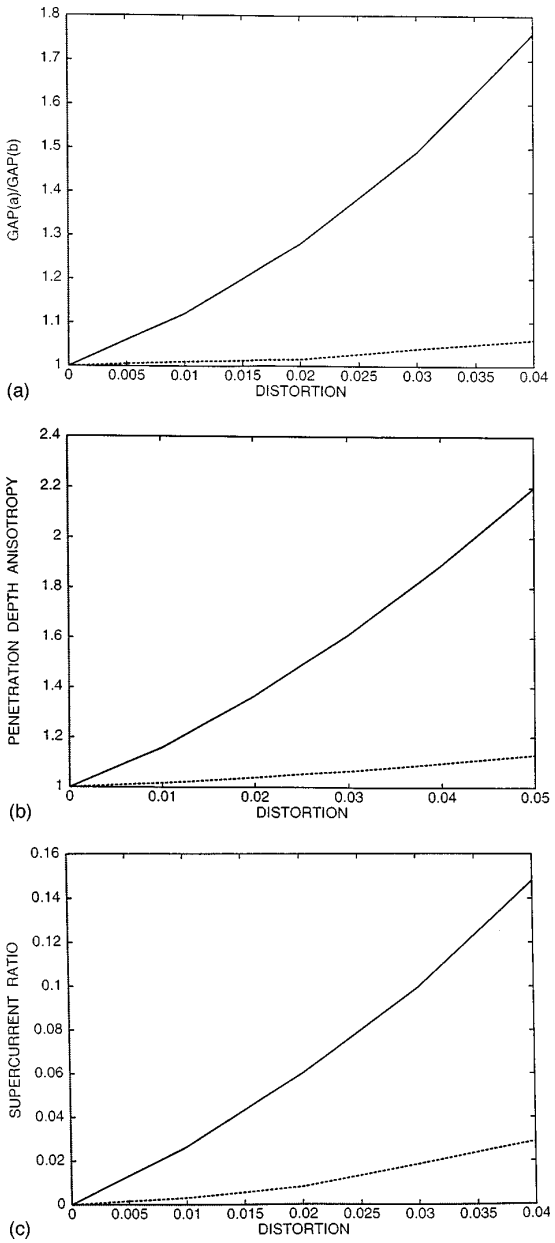

FIG. 15. Comparison of the effect of orthorhombicity in the MD regime and in spin-fluctuation-mediated superconductivity. (a) The ratio of the gaps along the *a* and *b* directions Δ_a^2/Δ_b^2 as a function of the distortion parameter β. (b) The London penetration depth in-plane anisotropy λ_b^2/λ_a^2 as a function of the distortion parameter β. (c) The ratio of supercurrent obtained from a Josephson junction of Pb with anisotropic Y-Ba-Cu-O over that expected from a junction of lead with isotropic Y-Ba-Cu-O with gap magnitude $(1/2)(|\Delta_a|+|\Delta_b|)$. In all cases the full lines correspond to the MD regime as described in the text, while dashed lines correspond to the MMP effective scattering amplitude [Eq. (33)] with the same dispersion conditions.

the corresponding β dependence of Δ_a^2/Δ_b^2. The structural distortion of the CuO_2 planes induces a distortion in the superconductive behavior that is an order of magnitude larger in the case of MD compared to that in the case of spin-fluctuation scattering.[46] In the latter case, the orthorhombically induced ''distortion'' in superconductivity is on the order of the distortion introduced in the tight-binding dispersion and therefore of the structural distortion.

The experiments in Y-Ba-Cu-O suggest strong orthorhombicity effects that could exclude spin fluctuations if only the in-plane electronic physics is relevant and indicate that MD is at the origin of anisotropy. In fact, let us consider the London penetration depth along the two different directions at zero temperature

$$\lambda_{k_x(k_y)}^{-2} \propto \sum_{\mathbf{k}} v_{k_x(k_y)}^2 [\partial f(E_{\mathbf{k}})/\partial E_{\mathbf{k}}], \tag{34}$$

where $E_{\mathbf{k}}=\sqrt{\xi_{\mathbf{k}}^2+\Delta_{\mathbf{k}}^2}$ and v_{k_i} are the Fermi velocities along k_x and k_y. The experimental results of Ref. 93 indicate large in-plane anisotropy of the penetration depth $\lambda_a/\lambda_b \approx 1.6$. We show in Fig. 15(b) the dependence of the in-plane penetration depth anisotropy $\lambda_b^{-2}/\lambda_a^{-2}$ on the distortion parameter β. The full line corresponds to the MD regime, while the dashed line to the MMP spin-fluctuation scattering. We see that, in the MD regime, the in-plane distortion could be sufficient to produce the experimental in-plane anisotropy of the penetration depth for realistic values of the in-plane distortion parameter $\beta \approx 0.04$. On the other hand, using MMP interaction, the reported in-plane anisotropy of λ for the same distortion parameter β is an order of magnitude smaller than in the experiment.

The same conclusion is derived from the c-axis Josephson tunneling results of Sun *et al.*[84] In fact they observed Josephson tunneling currents on c-axis Pb/insulator/$YBa_2Cu_3O_7$ tunnel junctions. According to the analysis of Ambegaokar and Baratoff[96] the Josephson effect is described by

$$JR=\frac{2\pi T}{N_1 N_2}\frac{1}{\pi}\sum_{n=0}^{\infty}\sum_{\mathbf{k}}\frac{\Delta_1(\mathbf{k})}{\xi_1(\mathbf{k})^2+\Delta_1(\mathbf{k})^2+\omega_n^2} \times \sum_{\mathbf{k}'}\frac{\Delta_2(\mathbf{k}')}{\xi_2(\mathbf{k}')^2+\Delta_2(\mathbf{k}')^2+\omega_n^2}. \tag{35}$$

At zero temperature the sum over the fermion Matsubara frequencies becomes an integral that can be performed straightforwardly, leading to the following expression for the Josephson current J at $T=0$:

$$J(T=0)R=\frac{1}{2\pi}\frac{1}{N_1 N_2}\sum_{\mathbf{k}\mathbf{k}'}\Delta_1(\mathbf{k})\Delta_2(\mathbf{k}') \times\frac{1}{\sqrt{\xi_1(\mathbf{k})^2+\Delta_1(\mathbf{k})^2}\sqrt{\xi_2(\mathbf{k}')^2+\Delta_2(\mathbf{k}')^2}} \times\frac{1}{\sqrt{\xi_1(\mathbf{k})^2+\Delta_1(\mathbf{k})^2}+\sqrt{\xi_2(\mathbf{k}')^2+\Delta_2(\mathbf{k}')^2}}, \tag{36}$$

where R is the junction resistance and $N_i(0)$ is the densities of states on the Fermi level. It is clear that if Δ_1 and Δ_2 are orthogonal (they belong to different irreducible representations of the point group), there should not be any Josephson current in the junction. Therefore, since the gap of Pb is known to be s wave, the observation of the Josephson current seems to exclude a purely d-wave gap in Y-Ba-Cu-O and a significant part of the s component is necessary in order to have Josephson coupling between the two condensates.

For the Pb/insulator/Y-Ba-Cu-O junction, if we suppose that the Pb gap is isotropic then in Eq. (35) the sum over k for the isotropic case becomes trivial leading to a term proportional to the density of states of lead. At zero temperature the Matsubara frequency sum becomes a frequency integral taking here the form $\int_0^\infty d\omega F(\omega)G(\omega)$ where $F(\omega)=(\Delta_{\mathrm{Pb}}^2+\omega^2)^{-1/2}$ and $G(\omega)=[\xi_{\mathrm{Y}}(\mathbf{k})^2+\Delta_{\mathrm{Y}}(\mathbf{k})^2+\omega^2]^{-1}$. This last integral is calculated numerically. The index Y stands for the gap and dispersion of Y-Ba-Cu-O and the index Pb for the gap of lead. If Δ_{Y} were also isotropic and the band of Y-Ba-Cu-O were also isotropic and infinite one should recover the classical Ambegaokar and Baratoff result for a Josephson junction between isotropic superconductors

$$J(T=0)R=\frac{2\Delta_{\mathrm{Pb}}\Delta_{\mathrm{Y}}}{\Delta_{\mathrm{Pb}}+\Delta_{\mathrm{Y}}}K\left[\left|\frac{\Delta_{\mathrm{Pb}}-\Delta_{\mathrm{Y}}}{\Delta_{\mathrm{Pb}}+\Delta_{\mathrm{Y}}}\right|\right], \tag{37}$$

with K a complete elliptic integral of the first kind.

In Ref. 84 a supercurrent along the c axis of a Pb/insulator/Y-Ba-Cu-O junction was observed. This supercurrent was about 10% of what should be expected from the isotropic Ambegaokar-Baratoff formula (for Y-Ba-Cu-O the gaps were taken equal to $1.76T_c$ as expected in weak-coupling BCS theory). As we noticed, the presence of the supercurrent demonstrates already that an s component is present in the gap of Y-Ba-Cu-O. However, the weakness of the supercurrent could show that the d components are nevertheless dominant.[97] In our approach, the gap in Y-Ba-Cu-O is indeed dominantly d wave for the reasons we discussed in Sec. VII A yet because of the orthorhombic distortion there is also an s component that is responsible for the Josephson coupling with the condensate of lead. To show that this approach could reasonably account for the results of Ref. 84 we take two different cases. In the first case we consider that the gap of Y-Ba-Cu-O is isotropic and in the second case we obtain the gap from the solution of the BCS equations as before. In both cases we adjust the Y-Ba-Cu-O gap to a value about 15 times larger than the gap of Pb. We also adjust the isotropic gap taken for Y-Ba-Cu-O in the first case to be equal to $(1/2)(|\Delta_a|+|\Delta_b|)$ where Δ_a and Δ_b are the gap magnitudes we obtain along a and b, respectively, [as we show in Fig. 15(a) the gap changes not only its sign but also its magnitude by a $\pi/2$ rotation]. What would be comparable to the findings of Ref. 84 is the ratio of the Josephson supercurrent produced using the anisotropic gap we obtain in the MD regime solving the BCS equations as previously, over the supercurrent obtained in the isotropic case and which should correspond to the Ambegaokar-Baratoff expectations. We plot in Fig. 15(c) the evolution of this ratio with the distortion parameter β. When $\beta=0$ we have no supercurrent but as the distortion parameter reaches values as high as $\beta=0.04$ we obtain appreciable currents of the order of 15% of what should be expected in a junction between isotropic superconductors, in good agreement with the results of Ref. 84. The dashed line in Fig. 15(c) shows the evolution of the same ratio with β but when the anisotropic Y-Ba-Cu-O gap is obtained using the MMP interaction. For the supercurrent also, the orthorhombicity effect is about an order of magni-

tude larger in the case of MD than in the case of the MMP interaction. The supercurrent obtained using the MMP interaction can never reproduce the experimental reports and involving the chains is unavoidable in that case.

It emerges therefore a fundamental qualitative difference between MD and anisotropic scattering with spin fluctuations. In the case of anisotropic scattering, if the orthorhombic distortions interpretation of the *s* and *d* mixing in Y-Ba-Cu-O makes sense, then the chains should necessarily participate fundamentally in the pairing and at least about 25% of the condensate should be located there. In fact, with a distortion factor of 25% ($\beta=0.25$) Carbotte and collaborators[91] were able to reproduce various characteristics of the *ab* anisotropy in $YBa_2Cu_3O_7$ using the MMP interaction. Of course $\beta=0.25$ is not physical for the CuO_2 plane distortion, but was used by the authors as an approximate approach in order to simulate the effect of the Cu-O chains within a one-band picture without considering explicitly the chain band. Our analysis suggests that if instead of the MMP interaction [Eq. (33)] one considers the effective interaction we obtained near the PS instability given in Eq. (28), we obtain the same magnitude of orthorhombicity effects but for the realistic CuO_2 plane value of $\beta\approx0.04$. The orthorhombic distortion of the planes could therefore be sufficient and the chains irrelevant.

VIII. EPILOGUE

We presented in this manuscript a paradigm in which superconductivity mediated by isotropic electron-phonon scattering can have very unconventional properties usually attributed to exotic pairing mechanisms. For the occurrence of this type of ''unconventional'' superconductivity short-range (in real space) Coulomb correlations like in the Hubbard models are necessary. Such a system can be driven to a phase separation instability even by phonons. Approaching the instability line from the Fermi-liquid side, results in a strong enhancement of long-wavelength electron-phonon scattering. Dominance of long-wavelength processes leads to momentum decoupling in superconductivity which is a tendency of decorrelation of the superconductive behavior in the various regions of the Fermi surface. We have discussed the original qualitative aspects of this type of unconventional superconductivity that arises in the momentum decoupling regime.

We have particularly emphasized the qualitative aspects that may differentiate this new type of unconventional superconductivity from other mechanisms of unconventional superconductivity proposed earlier which involve anisotropic scattering for example with spin fluctuations. We identified some relevant original qualitative aspects of MD that may help identifying the origin of unconventional superconductivity. Such aspects are the very small dependence of the condensation free energy on the gap symmetry which could be determined by the conventional (and marginal for the pairing) Coulomb pseudopotential, the temperature dependence of the shape of the anisotropy, and a large sensitivity of the order parameter to orthorhombic distortions. We have discussed these aspects in relation with the phenomenology of the high-T_c oxides showing that many puzzles are simple consequences of MD. We hope the reader is convinced that MD deserves serious consideration in the analysis of the superconducting phenomenology of the oxides, and *phonons remain serious candidates for the role of the mediators of the pairing*.

We must insist that, while we claim demonstration that phonons remain in the list of candidates for the pairing, we are very far from demonstrating their relevance. MD might not be automatically associated to phonon-mediated superconductivity close to a phase separation. There are other proposed mechanisms for high-T_c which also lead to MD. The most famous are the charge-transfer resonance mechanism of Littlewood, Varma, and Abrahams[20] which involves the long-wavelength process,[21] and the interlayer tunneling mechanism of Anderson and Chakravarty,[19] which corresponds effectively to $q\approx0$ pairing between the planes. In this paper, we provided the elements which may help distinguish MD from anisotropic scattering, for example, with spin fluctuations. In a future paper, we will attempt a finer analysis with the objective to identify qualitative aspects that could help to distinguish between the (proposed in this paper) phonon mechanism near a PS instability and the models of Refs. 20, 21, and 19.

The contribution of this paper in the discussion around the high-T_c phenomenon can therefore be summarized as follows:

(a) We add support to the idea that phonons could be mediators of a type of unconventional superconductivity in the oxides.

(b) We provide elements for distinguishing this type of unconventional superconductivity from the older types based for example on spin fluctuations pairing.

(c) We identify unexpected qualitative implications of other models that have been proposed[20,21,19] to explain high-T_c superconductivity in the cuprates.

In the discussion of our findings we focus on the behavior of the high-T_c oxides. We feel, nevertheless, convinced that our analysis may constitute a basis for a serious reconsideration of our ideas on other so-called ''unconventional superconductors'' like the heavy fermion and organic superconductors, restoring for example phonons in the list of the potential mediators of the pairing there also.

ACKNOWLEDGMENTS

I am grateful to Professor E. N. Economou and Dr. J. Giapintzakis for numerous stimulating discussions and a critical reading of the manuscript. Also, it is a pleasure to acknowledge valuable discussions with Marshall Onellion, Christophe Renner, Zhixun Shen, Marko Grilli, Claudio Castellani, Gregory Psaltakis, Nicos Papanicolaou, Thimios Liarokapis, Luciano Pietronero, Emanuelle Cappelluti, Andrea Perali, and Martin Peter.

*Electronic address: varelogi@iesl.forth.gr

[1] E. Manousakis, Rev. Mod. Phys. **63**, 1 (1991).
[2] E. Dagotto, Rev. Mod. Phys. **66**, 763 (1994).
[3] A. Georges *et al.*, Rev. Mod. Phys. **68**, 13 (1996).
[4] M. Arai *et al.*, Phys. Rev. Lett. **69**, 359 (1992); H. A. Mook *et al.*, *ibid.* **69**, 2272 (1992); N. Pyka *et al.*, *ibid.* **70**, 1457 (1993).
[5] R. M. Mcfarlane *et al.*, Solid State Commun. **63**, 831 (1987); A. Wittlin *et al.*, *ibid.* **64**, 477 (1987); R. Zeyher and G. Zwicknagl, Z. Phys. B **78**, 175 (1990).
[6] D. Zech *et al.*, Nature (London) **371**, 681 (1994).
[7] R. Aoki *et al.*, Physica C **225**, 1 (1994).
[8] G. Varelogiannis and L. Pietronero, Phys. Rev. B **52**, R15 753 (1995).
[9] J. H. Kim *et al.*, Phys. Rev. B **44**, 5148 (1991).
[10] K. J. von Szczepanski and K. W. Becker, Z. Phys. B **89**, 327 (1992).
[11] J. H. Kim and Z. Tesanovic, Phys. Rev. Lett. **71**, 4218 (1993).
[12] A. A. Abrikosov, Physica C **222** 191 (1994); Physica C **244**, 243 (1995).
[13] U. Trapper *et al.*, Z. Phys. B **93**, 465 (1994).
[14] M. L. Kulic and R. Zeyher, Phys. Rev. B **49**, 4395 (1994).
[15] M. Grilli and C. Castellani, Phys. Rev. B **50**, 16 880 (1994).
[16] G. Varelogiannis, Phys. Rev. B **50**, 15 974 (1994).
[17] G. Varelogiannis, Physica C **249**, 87 (1995); R. Combescot and G. Varelogiannis, J. Low Temp. Phys. **102**, 193 (1996).
[18] A. W. Overhauser, Phys. Rev. B **3**, 1888 (1971).
[19] S. Chakravarty *et al.*, Science **261**, 337 (1993).
[20] P. B. Littlewood, C. M. Varma, and E. Abrahams, Phys. Rev. Lett. **63**, 2602 (1989).
[21] P. B. Littlewood, Phys. Rev. B **42**, 10 075 (1990).
[22] H. Krakauer, W. E. Pickett, and R. E. Cohen, Phys. Rev. B **47**, 1002 (1993).
[23] D. M. Newns *et al.*, Phys. Rev. B **43**, 3075 (1993); R. S. Markiewicz, Physica C **217**, 381 (1993).
[24] G. Varelogiannis and E. N. Economou, Europhys. Lett. **43**, 313 (1998).
[25] J. P. Franck, in *Physical Properties of High-T_c Superconductors IV*, edited by D. M. Ginsberg (World Scientific, Singapore, 1994), p. 189.
[26] T. Dahm *et al.*, Phys. Rev. B **54**, 12 006 (1996).
[27] J. E. Hirsch *et al.*, Phys. Rev. Lett. **60**, 1668 (1988); Phys. Rev. B **39**, 243 (1989).
[28] S. Trugman, Phys. Scr. **T27**, 113 (1989).
[29] M. Marder, N. Papanicolaou, and G. C. Psaltakis, Phys. Rev. B **41**, 6920 (1990).
[30] V. J. Emery, S. A. Kivelson, and Q. Lin, Phys. Rev. Lett. **64**, 475 (1990).
[31] A. N. Andriotis *et al.*, Phys. Rev. B **47**, 1002 (1993).
[32] G. Kotliar and A. E. Ruckenstein, Phys. Rev. Lett. **57**, 1362 (1986).
[33] V. I. Anisimov, J. Zaanen, and O. K. Andersen, Phys. Rev. B **44**, 943 (1991).
[34] For a review see, W. Pickett, Rev. Mod. Phys. **61**, 433 (1989).
[35] P. Fulde, *Electron Correlations in Molecules and Solids*, 2nd ed. Springer Series in Solid State Sciences, Vol. 100 (Springer-Verlag, Berlin, 1993).
[36] J. Kanamori, Prog. Theor. Phys. **30**, 275 (1963).
[37] J. R. Schrieffer and P. A. Wolff, Phys. Rev. **149**, 491 (1966).
[38] C. Kane, P. A. Lee, and N. Read, Phys. Rev. B **39**, 6880 (1989); S. Trugman, Phys. Rev. B **41**, 892 (1990); E. Dagotto *et al.*, *ibid.* **41**, 2585 (1990); P. Prelovšek, I. Sega, and J. Bonča, *ibid.* **42**, 10 706 (1990).
[39] D. Poilblanc *et al.*, Phys. Rev. B **47**, 5984 (1993).
[40] P. B. Littlewood, C. M. Varma, and E. Abrahams, Phys. Rev. Lett. **60**, 379 (1987).
[41] O. K. Andersen *et al.*, Phys. Rev. B **49**, 4145 (1994).
[42] C. Castellani, C. Di Castro, and M. Grilli, Phys. Rev. Lett. **75**, 4650 (1995).
[43] J. Zaanen *et al.*, Phys. Rev. Lett. **60**, 2685 (1988).
[44] E. N. Economou and C. T. White, Phys. Rev. Lett. **38**, 289 (1977); R. DeMarco, E. N. Economou, and D. C. Licciardello, Solid State Commun. **21**, 687 (1977); E. N. Economou, C. T. White, and R. R. DeMarco, Phys. Rev. B **18**, 3946 (1978); **18**, 3968 (1978).
[45] E. N. Economou, *Green's Functions in Quantum Physics* (Springer-Verlag, Heidelberg, 1983).
[46] A comparative study of spin-fluctuation pairing versus momentum decoupling for the superconducting phenomenology of the oxides will be given in another paper.
[47] J. Ma *et al.*, Science **267**, 862 (1995).
[48] G. Varelogiannis *et al.*, Phys. Rev. B **54**, R6877 (1996).
[49] D. A. Wollman *et al.*, Phys. Rev. Lett. **71**, 2134 (1993); D. A. Brawner and H. R. Ott, Phys. Rev. B **50**, 6530 (1994); C. C. Tsuei *et al.*, Phys. Rev. Lett. **73**, 593 (1994).
[50] W. N. Hardy *et al.*, Phys. Rev. Lett. **70**, 3999 (1990); L. A. de Vaulchier *et al.*, Europhys. Lett. **33**, 153 (1996).
[51] Some proposed models describe the phase sensitive and node sensitive experiments in $YBa_2Cu_3O_7$ without *d* waves. See, e.g., R. A. Clemm and S. H. Liu, Phys. Rev. Lett. **74**, 2343 (1995).
[52] P. Chaudhari and S.-Y. Lin, Phys. Rev. Lett. **72**, 1084 (1994).
[53] For reviews see R. C. Dynes, Solid State Commun. **92**, 53 (1994); J. R. Schrieffer, *ibid.* **92**, 129 (1994); J. Annett, N. Goldenfeld, and A. J. Leggett, in *Physical Properties of High-T_c Superconductors*, edited by D. M. Ginsberg (World Scientific, Singapore, 1996), Vol. VI; J. Low Temp. Phys. **105**, 473 (1996).
[54] Z.-X. Shen *et al.*, Phys. Rev. Lett. **70**, 1553 (1993).
[55] Z.-X. Shen and D. S. Dessau, Phys. Rep. **253**, 1 (1995).
[56] H. Ding *et al.*, Phys. Rev. B **54**, R9678 (1996).
[57] R. J. Kelley *et al.*, Science **271**, 1255 (1996).
[58] C. Kendziora, R. J. Kelley, and M. Onellion, Phys. Rev. Lett. **77**, 727 (1996).
[59] B. L. Altshuler, L. B. Ioffe, and A. J. Millis, Phys. Rev. B **53**, 415 (1996). We thank Andy Millis for bringing this reference to our attention and for a stimulating discussion.
[60] G. Santi *et al.*, J. Supercond. **8**, 225 (1995).
[61] B. E. C. Koltenbach and R. Joynt, Rep. Prog. Phys. **60**, 23 (1997).
[62] C. S. Hellberg and E. Manousakis, Phys. Rev. B **52**, 4639 (1995).
[63] A. Nazarenko and E. Dagotto, Phys. Rev. B **53**, R2987 (1996).
[64] J. Song and J. Annett, Phys. Rev. B **51**, 3840 (1995).
[65] H. Kamimura *et al.*, Phys. Rev. Lett. **77**, 723 (1996).
[66] A. Perali *et al.*, Phys. Rev. B **54**, 16 216 (1996).
[67] P. B. Allen and B. Mitrovic, in *Solid State Physics: Advances in Research and Applications* (Academic, New York, 1981), Vol. 37.
[68] J. P. Carbotte, Rev. Mod. Phys. **62**, 1027 (1990).
[69] J. Bardeen and M. Stephen, Phys. Rev. **136**, A1485 (1964).
[70] J. R. Schrieffer, *Theory of Superconductivity*, Frontiers in Physics (Benjamin, New York, 1964).
[71] J. Betouras and R. Joynt, Europhys. Lett. **31**, 119 (1995).
[72] G. Varelogiannis, Physica C **232**, 49 (1994).

[73] P. W. Anderson, Phys. Rev. Lett. **67**, 660 (1991); A. S. Alexandrov and J. Ranninger, Physica C **198**, 360 (1992); P. B. Littlewood and C. M. Varma, Phys. Rev. B **46**, 405 (1992).
[74] G. Varelogiannis, Physica C **235-240**, 2381 (1994).
[75] G. Varelogiannis, Phys. Rev. B **51**, R1381 (1995); Phys. Rev. Lett. **76**, 3236 (1996).
[76] G. Varelogiannis, Z. Phys. B **104**, 411 (1997).
[77] A detailed analysis of the dip anisotropy and asymmetry along the lines of Ref. 75 is given in G. Varelogiannis (unpublished).
[78] O. V. Dolgov, A. A. Golubov, and A. E. Koshelev, Solid State Commun. **72**, 81 (1989); L. Coffey, Phys. Rev. Lett. **64**, 1071 (1991).
[79] P. B. Allen and D. Rainer, Nature (London) **349**, 396 (1991).
[80] R. Combescot and G. Varelogiannis, Europhys. Lett. **17**, 625 (1992).
[81] See, e.g., D. Mandrus *et al.*, Nature (London) **351**, 460 (1991).
[82] See, e.g., Y. Hwu *et al.*, Phys. Rev. Lett. **67**, 2573 (1991).
[83] Ch. Renner and Ø. Fischer, Phys. Rev. B **51**, 9208 (1995).
[84] A. G. Sun *et al.*, Phys. Rev. Lett. **72**, 2667 (1994).
[85] R. Kleiner *et al.*, Phys. Rev. Lett. **76**, 2161 (1996).
[86] A. G. Sun *et al.*, Phys. Rev. B **50**, 3266 (1994).
[87] K. A. Müller, Nature (London) **377**, 133 (1995).
[88] J. F. Annett, Adv. Phys. **39**, 83 (1990).
[89] K. Maki and N. T. Beal-Monod, Phys. Lett. A **208**, 365 (1995).
[90] S. V. Pokrovsky and V. L. Pokrovsky, Phys. Rev. Lett. **75**, 1150 (1995); Phys. Rev. B **54**, 13 275 (1996).
[91] C. O'Donovan *et al.*, Phys. Rev. B **51**, 6588 (1995); D. Branch and J. P. Carbotte, *ibid.* **52**, 603 (1995); J. M. Rendell and J. P. Carbotte, *ibid.* **53**, 5889 (1996).
[92] S. A. Sunshine *et al.*, Phys. Rev. B **38**, 893 (1988).
[93] K. Zhang, Phys. Rev. Lett. **73**, 2484 (1994).
[94] P. W. Anderson, Science **256**, 1526 (1992).
[95] A. J. Millis, H. Monien, and D. Pines, Phys. Rev. B **42**, 167 (1990).
[96] V. Ambegaokar and A. Baratoff, Phys. Rev. Lett. **10**, 486 (1963); **11**, 104 (1963).
[97] For the weakness of the supercurrent there are also alternative interpretations such as, for example, the possibility of *s*-wave gap in $YBa_2Cu_3O_7$ but significantly depleted in the external layer: M. Ledvij and R. A. Clemm, Phys. Rev. B **52**, 12 552 (1995).